

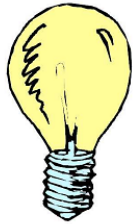


Physics and control of Edge Localized Modes (ELMs)

Valentin Igochine

Max-Planck Institut für Plasmaphysik
EURATOM-Association
D-85748 Garching bei München
Germany

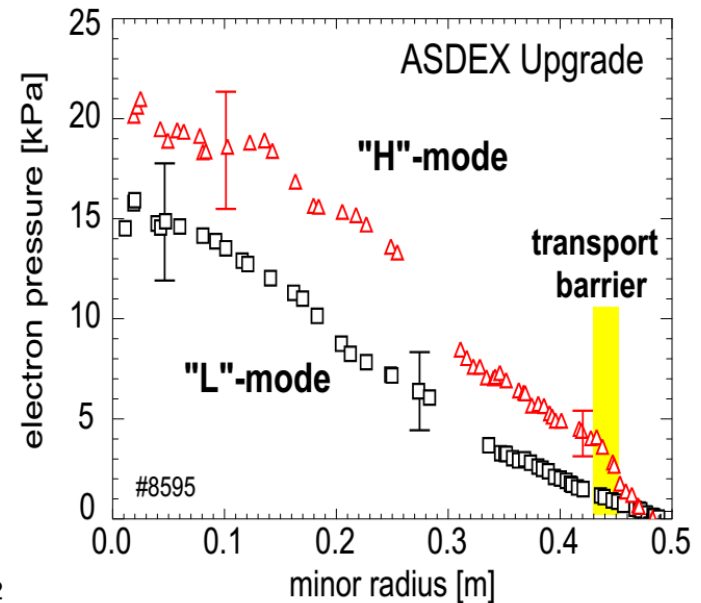
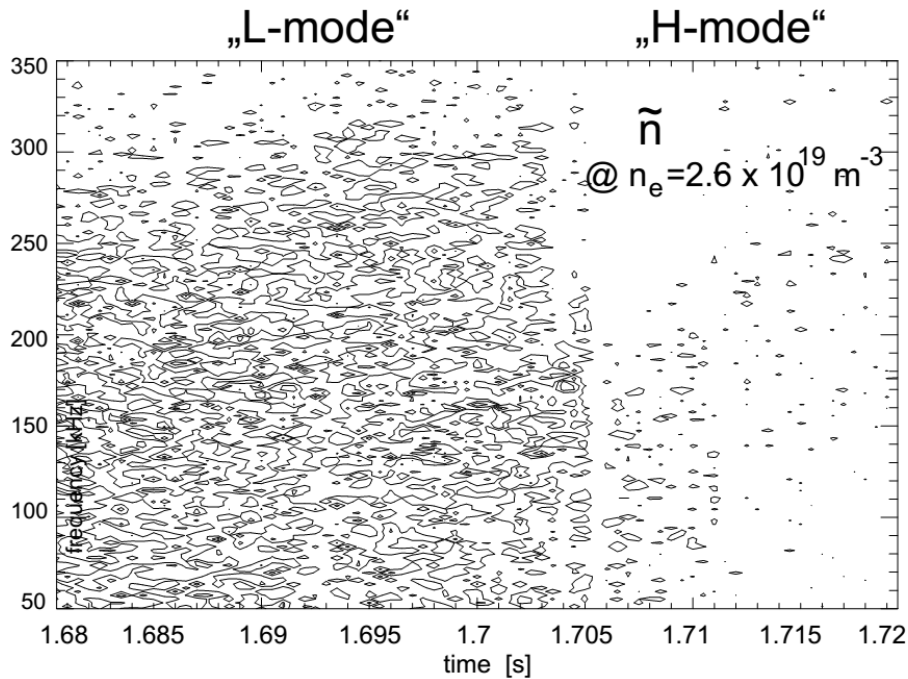
- Motivation
- Physics of ELMs
 - The trigger physics
 - ELM size and filament physics
 - Nonlinear behaviour of ELM
 - MHD modelling of ELMs
- Control of ELMs
 - Pellets
 - Gas puffing
 - Vertical kicks
 - Resonant Magnetic Perturbations
- Summary



Phase transition to high confinement regime (ASDEX 1984)

Reduced density fluctuation level

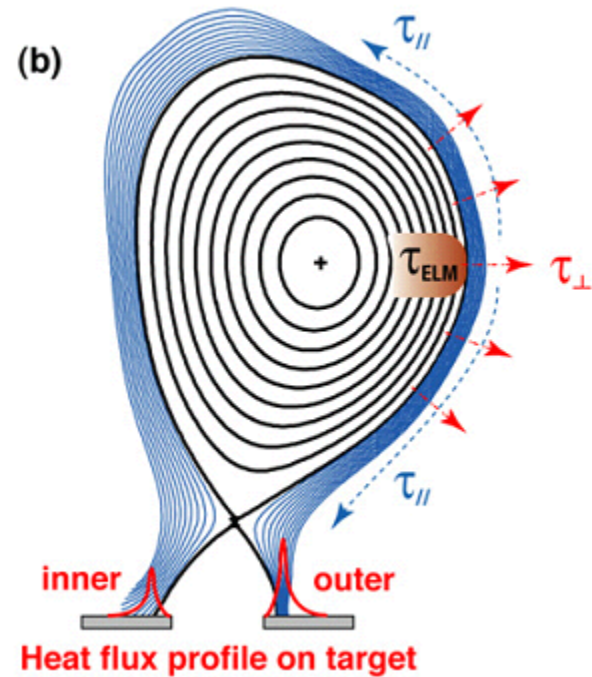
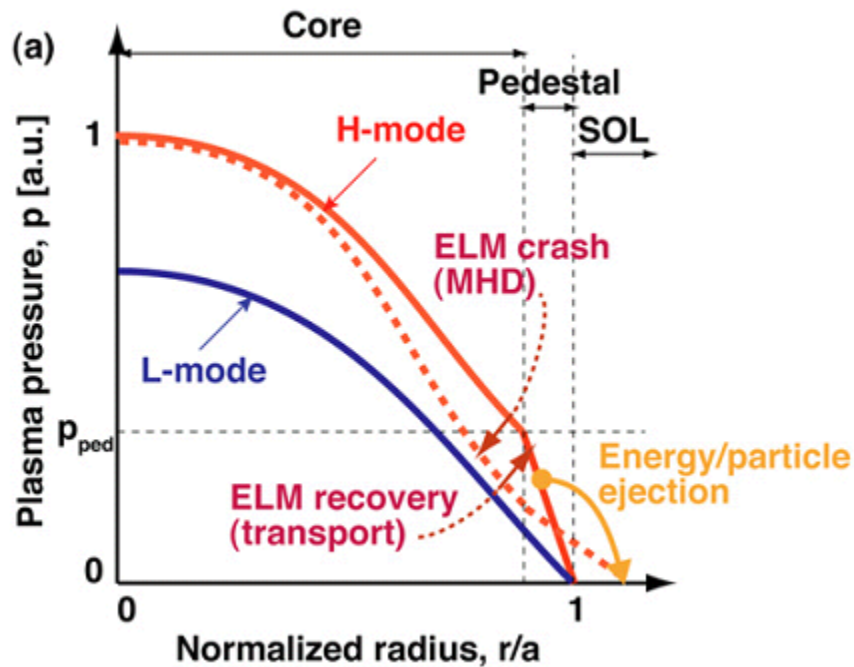
Reduced radial diffusivity
⇒ stronger pressure gradient



Typical H-mode signature is Edge Localized Modes (ELMs)

Schematic representation of the ELM cycle

Kamiya, PPCF, 2007



ELM crash, ejecting plasma energy/particle towards Scrape-Off-Layer (SOL)

Why is ELM control urgent for ITER?



Tungsten Erosion

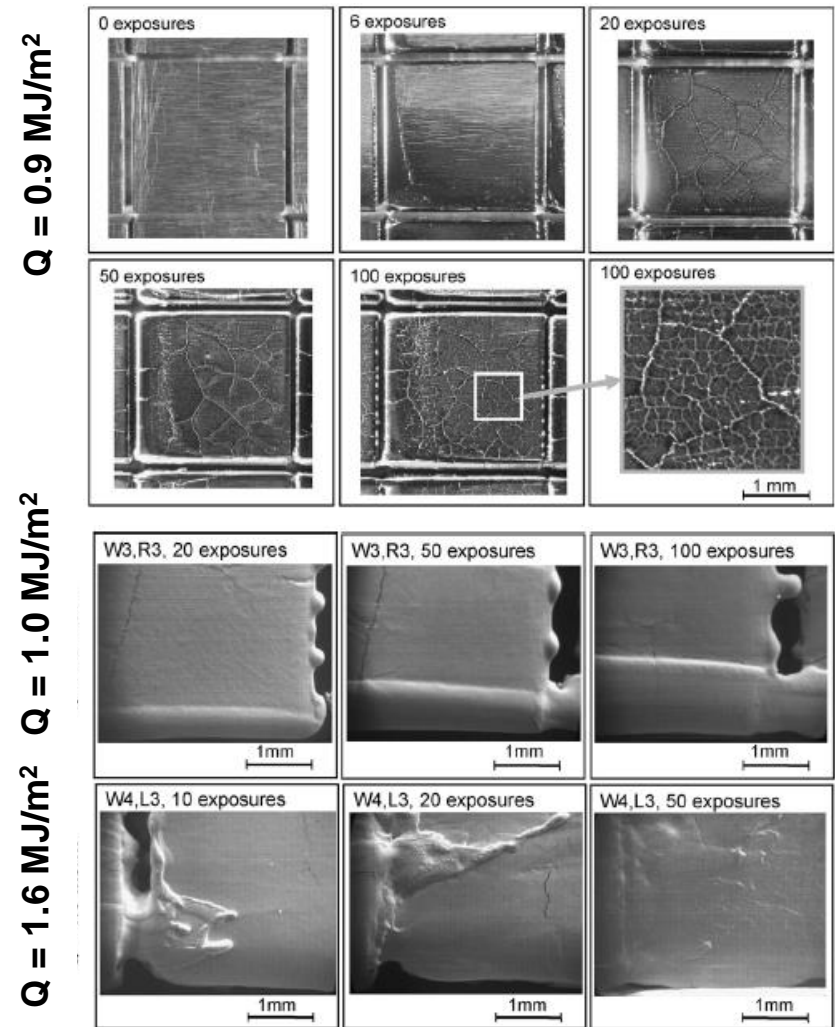
Tungsten melting, droplets, surface cracks if $W_{\text{ELM}} > 1\text{MJ}$.

... but predicted for large ELMs:
 $W_{\text{ELM,ITER}} \sim 30\text{MJ}$!

(ITER divertor life-time = only few shots with big ELMs!)

This requires a decrease in the 'natural' ELM size by a **factor of ~ 30**

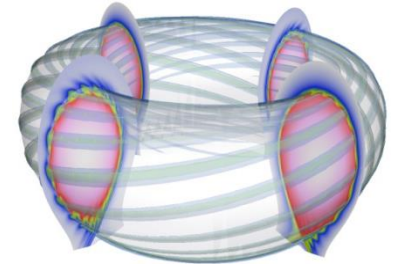
Zhitlukhin JNM 2007



ELM suppression/control is required for a steady state operation of ITER!

Physics of ELMs

Drives for instabilities in MHD are current and pressure profile gradients



Linearization:
 $A = A_0 + A_1$
 0 – equilibrium
 1 – perturbation

$$\delta W = \frac{1}{2} \int_{plasma} \left(\underbrace{\gamma p_0 (\nabla \cdot \vec{\xi})^2}_{>0} + (\vec{\xi} \cdot \nabla p_0) \nabla \cdot \vec{\xi} + \underbrace{\frac{B_1^2}{\mu_0}}_{>0} - \underbrace{\vec{j}_0 \cdot (\vec{B}_1 \times \vec{\xi})}_{\text{Current driven instabilities}} \right) d\tau + \underbrace{\int_{vacuum} \frac{B_{vac}^2}{2\mu_0}}_{>0} d\tau$$

Pressure driven instabilities
Current driven instabilities

Unstable only if $\delta W < 0$

Wesson, Tokamaks, 3rd Edition
 Freidberg, Ideal MHD

ELM trigger: ideal MHD



- It is widely believed that ideal MHD instabilities provide the trigger for the ELM
- Theoretically, the instability properties can be understood from δW for radial displacement, X , at large toroidal mode number, n :

$$\delta W = \pi \int_0^{\psi_a} d\psi \oint d\theta \left\{ \frac{JB^2}{R^2 B_p^2} |k_{\parallel} X|^2 + \frac{R^2 B_p^2}{JB^2} \left| \frac{1}{n} \frac{\partial}{\partial \psi} (JBk_{\parallel} X) \right|^2 \right.$$

Field-line bending:
strongly stabilising unless
 k_{\parallel} is small

$$\left. - \frac{2J}{B^2} \frac{dp}{d\psi} \left[|X|^2 \frac{\partial}{\partial \psi} \left(p + \frac{B^2}{2} \right) - \frac{i}{2} \frac{f}{JB^2} \frac{\partial B^2}{\partial \theta} \frac{X^*}{n} \frac{\partial X}{\partial \psi} \right] \right.$$

Pressure gradient/curvature
drive: destabilising if average
curvature is “bad”

$$\left. - \frac{X^*}{n} JBk_{\parallel} \left(\frac{\partial \sigma}{\partial \psi} X \right) + \frac{\partial}{\partial \psi} \left[\frac{\sigma}{n} X JBk_{\parallel}^* X^* \right] \right.$$

Current density gradient/edge
current drives kink/peeling
modes

σ =normalised current density

- Must ensure field-aligned perturbations or field line bending will suppress the instability: ideal MHD naturally produces filamentary structures

Kink or peeling modes



- A single, resonant Fourier mode

$$\delta W = \pi \int_0^{\psi_a} d\psi \oint d\theta \left\{ \frac{JB^2}{R^2 B_p^2} |k_{\parallel} X|^2 + \frac{R^2 B_p^2}{JB^2} \left| \frac{1}{n} \frac{\partial}{\partial \psi} (JBk_{\parallel} X) \right|^2 \right\}$$

Single Fourier mode, highly localised at rational surface eliminates field line bending

$$\frac{-2J}{B^2} \frac{dp}{d\psi} \left[|X|^2 \frac{\partial}{\partial \psi} \left(p + \frac{B^2}{2} \right) - \frac{i}{2} \frac{f}{JB^2} \frac{\partial B^2}{\partial \theta} \frac{X^*}{n} \frac{\partial X}{\partial \psi} \right]$$

$|X|^2$ constant around poloidal plane, so experiences “good” average curvature

⇒ Pressure gradient is stabilising

$$\left. - \frac{X^*}{n} JBk_{\parallel} \left(\frac{\partial \sigma}{\partial \psi} X \right) + \frac{\partial}{\partial \psi} \left[\frac{\sigma}{n} X JBk_{\parallel}^* X^* \right] \right\}$$

Driven unstable by current gradient at modest n : kink mode

Or edge current density at large n : peeling mode

- Peeling and kink modes are essentially the same thing
 - Driven by current density gradient, stabilised by pressure gradient
 - Highly localised

Ballooning modes



- Multiple Fourier modes couple to tap free energy of pressure gradient

$$\delta W = \pi \int_0^{\psi_a} d\psi \oint d\theta \left\{ \frac{JB^2}{R^2 B_p^2} |k_{\parallel} X|^2 + \frac{R^2 B_p^2}{JB^2} \left| \frac{1}{n} \frac{\partial}{\partial \psi} (JB k_{\parallel} X) \right|^2 \right.$$

To couple, each Fourier mode must extend across multiple rational surfaces:
Field line bending is minimised, but not eliminated

$$\frac{-2J}{B^2} \frac{dp}{d\psi} \left[|X|^2 \frac{\partial}{\partial \psi} \left(p + \frac{B^2}{2} \right) - \frac{i}{2} \frac{f}{JB^2} \frac{\partial B^2}{\partial \theta} \frac{X^*}{n} \frac{\partial X}{\partial \psi} \right]$$

Multiple Fourier modes couple to constructively interfere in bad curvature region: $|X|^2$ is maximum on outboard side

$$\left. - \frac{X^*}{n} JB k_{\parallel} \left(\frac{\partial \sigma}{\partial \psi} X \right) + \frac{\partial}{\partial \psi} \left[\frac{\sigma}{n} X JB k_{\parallel} X^* \right] \right\}$$

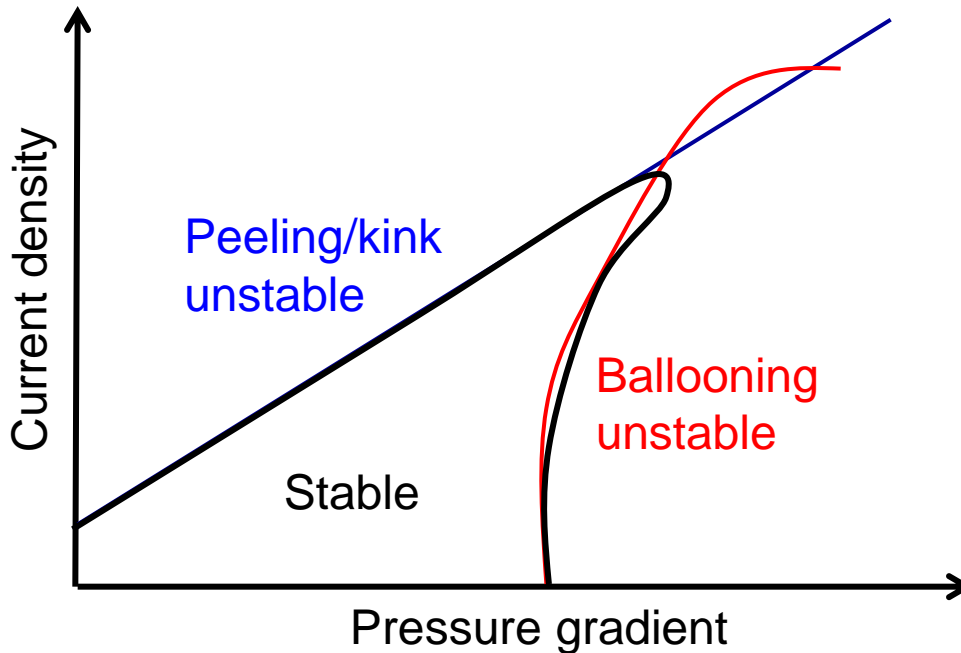
Current gradient does not play a role at large n ; edge current can influence mode

- Ballooning mode is unstable when the curvature exceeds field line bending
 - Critical $dp/d\psi$ is required (depends on shear, and therefore current)
 - Many coupled Fourier modes \Rightarrow radially extended mode structure

Ideal MHD stability diagram



- The peeling-ballooning mode stability diagram



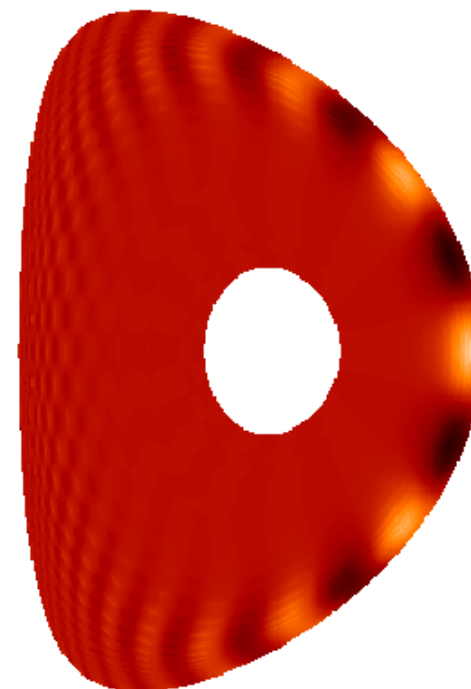
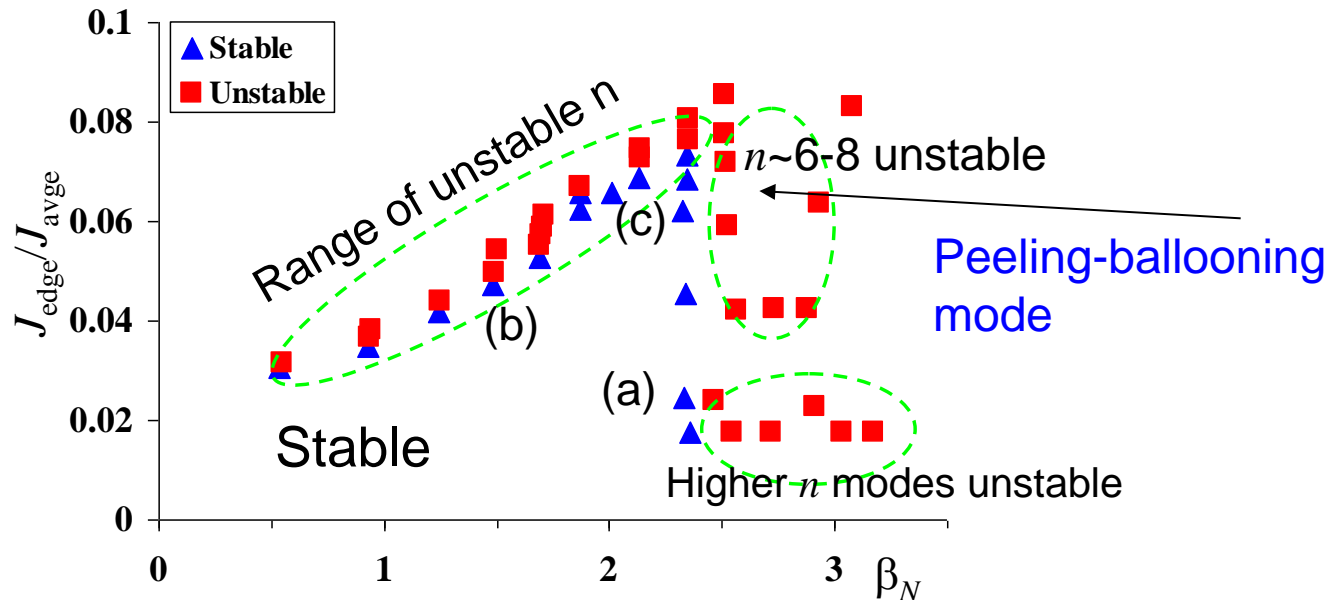
Important (slightly subtle) point

- Although stability diagrams are shown in terms of local dp/dr and J , profile effects cannot be neglected (when n is finite)
- Higher pressure gradient can be achieved for a narrower pedestal \Rightarrow care when interpreting experimental pedestal profiles

Ideal MHD stability diagram



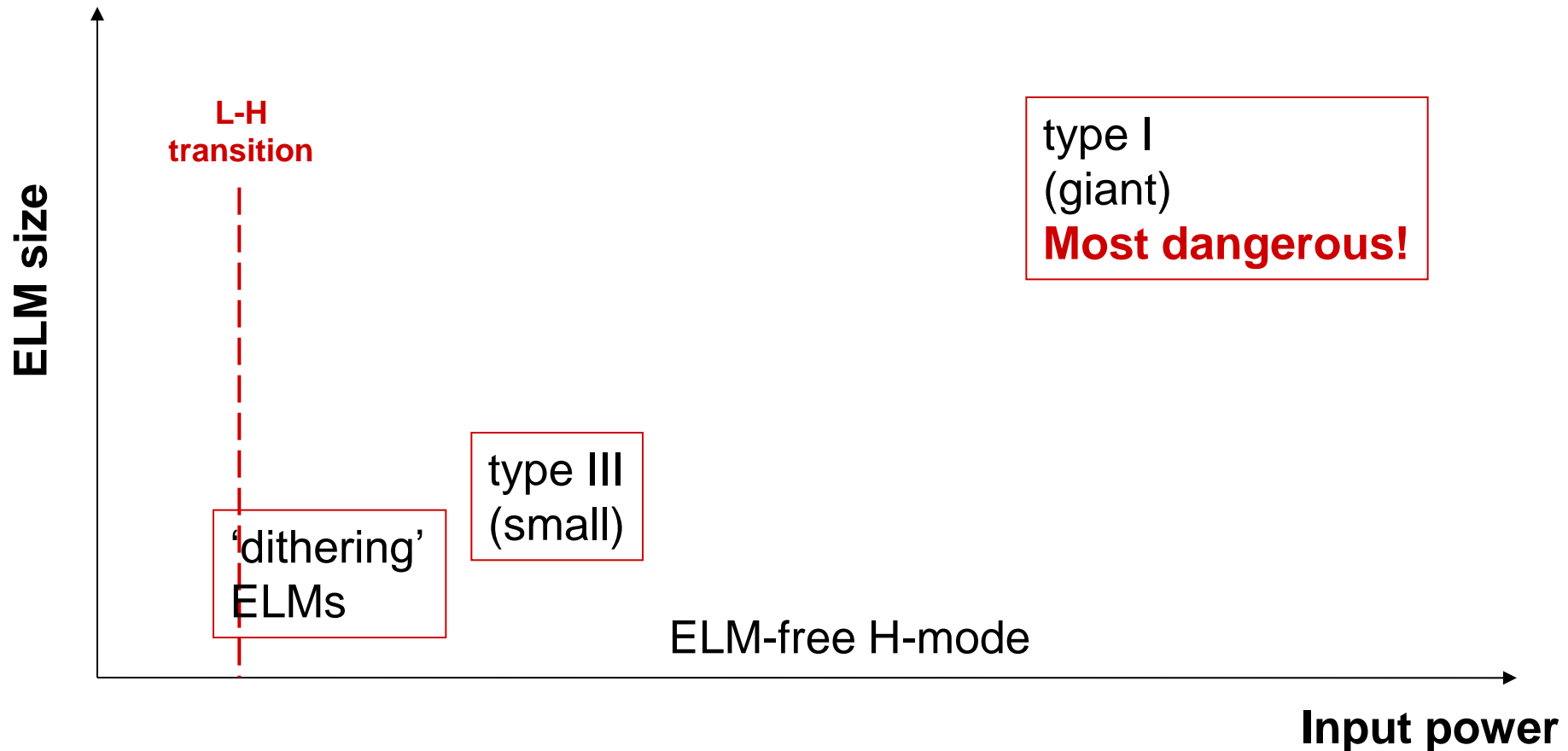
- Typical ELITE stability diagram (model JET-like equilibrium)



Types of ELMs



Definitions from Connor, PPCF, 98

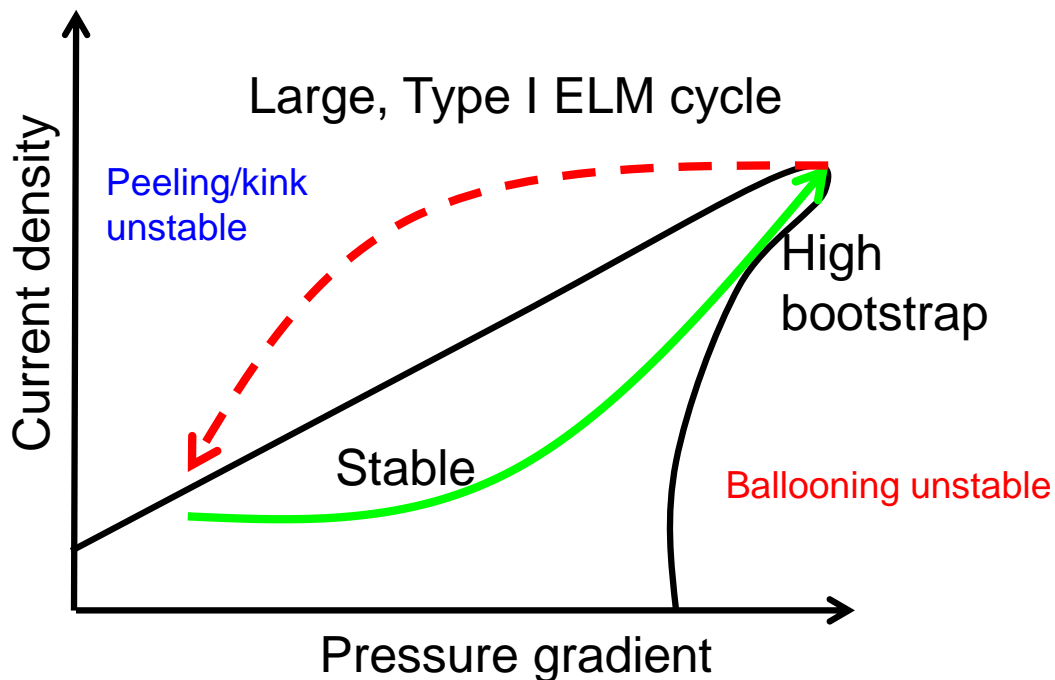


type II (or, sometimes, 'grassy') are associated with strongly-shaped tokamaks at high edge pressure when there is access to the second stability at the plasma edge

The ELM cycle: Type I



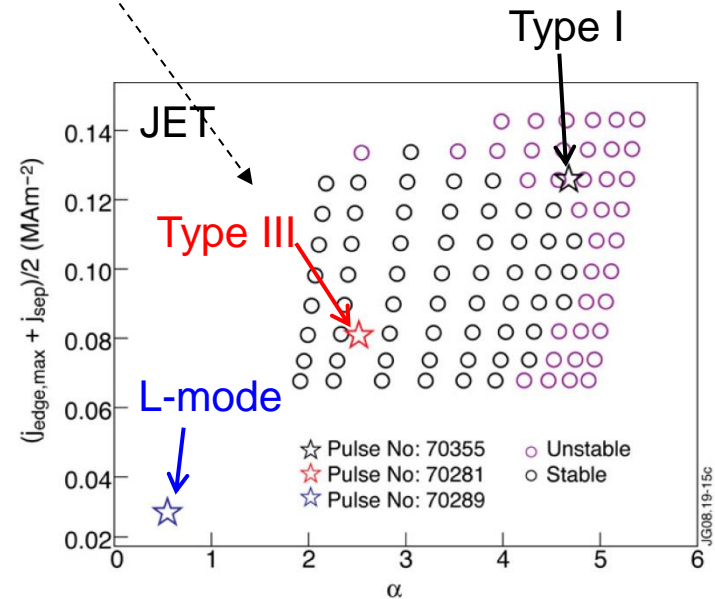
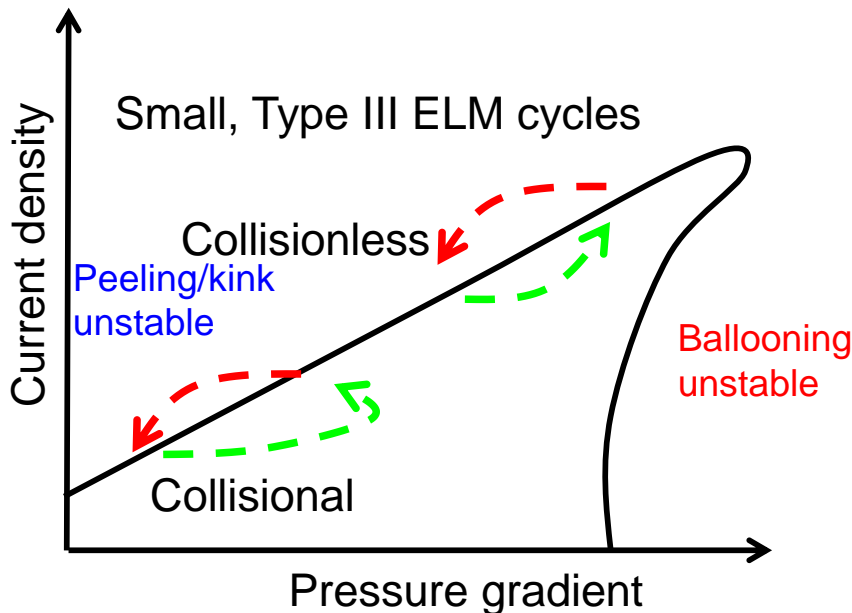
- Initial models: Type I ELM cycle
 - High pressure gradient in pedestal (so good performance)
 - Low collisionality, and strong bootstrap current
 - Extended linear mode across pedestal region
 - Anticipate a substantial crash



The ELM cycle: Type III



- Initial models: Type III ELMs (more speculative?)
 - Either highly collisional edge, destabilising resistive ballooning, driving pedestal to lower gradient and crossing peeling stability boundary
 - Or at higher temperatures, higher current pushes pedestal directly across peeling stability boundary
 - However, data seems to suggest Type III are stable to ideal modes (but uncertainty over edge current)

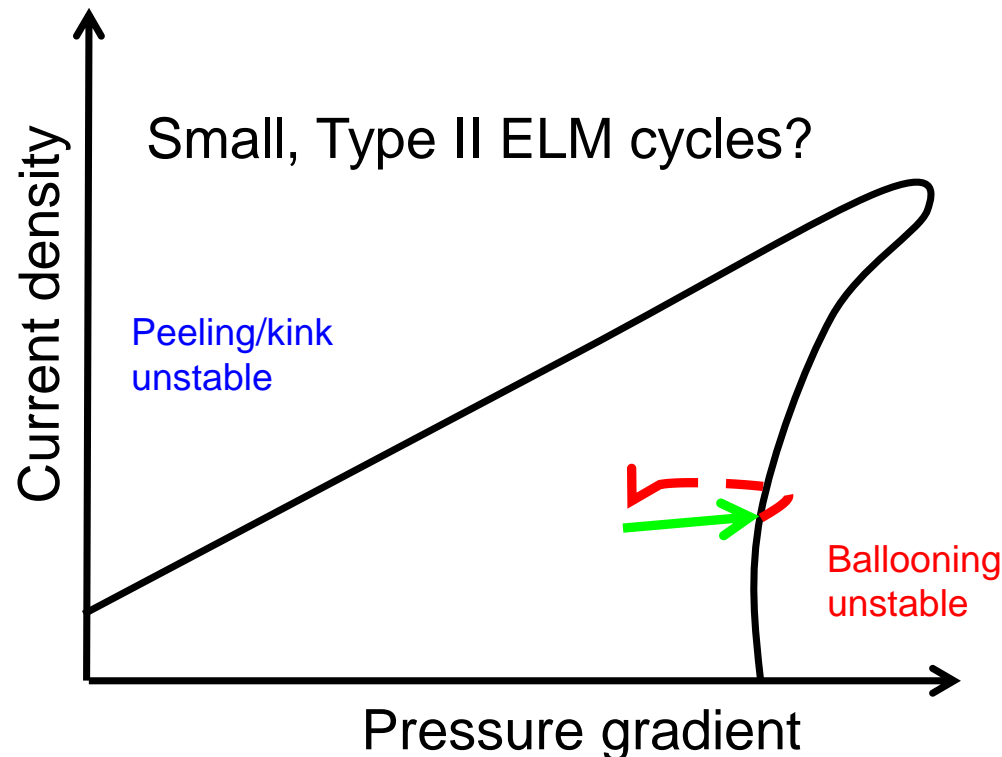


Saarelma, PPCF, 2009

The ELM cycle: Type II

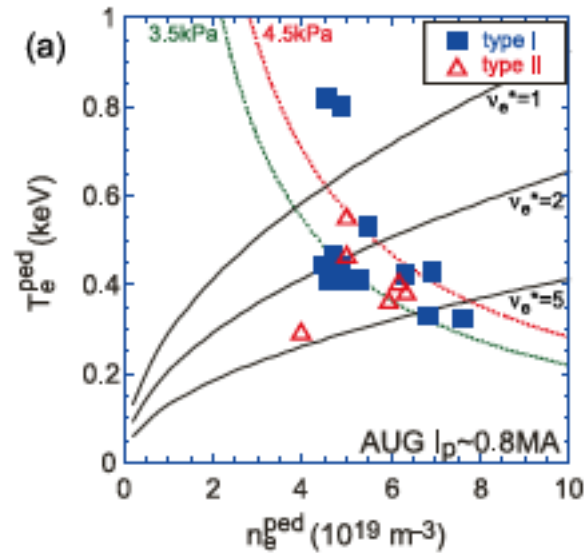
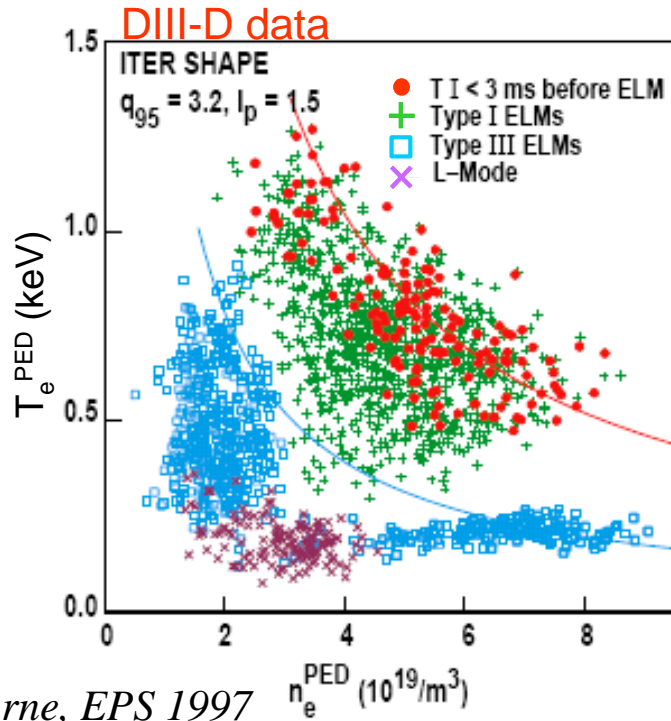


- Initial models: Type II ELMs (speculative, again)
 - Higher collisionality would help to suppress bootstrap current
 - Strong shaping can also push peeling boundary to high current density
 - Removes role of peeling mode, providing a pure ballooning mode

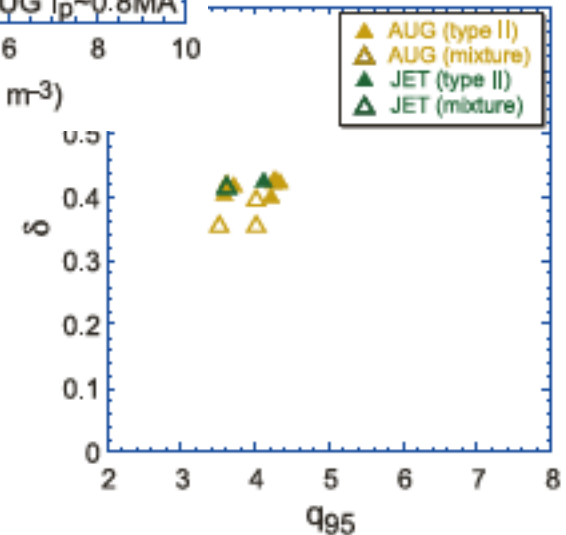


ELM Types: experiment

- The positions of Type I ELMs on an edge stability diagram are consistent with this picture:



Oyama, PPCF 2006

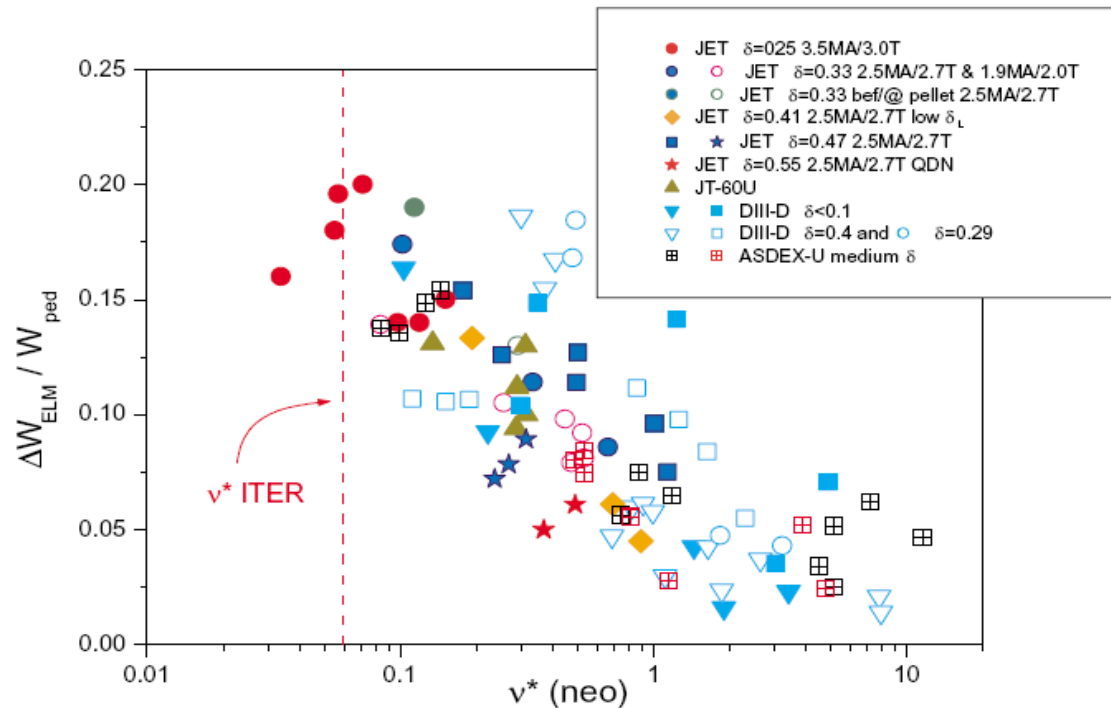


Existence space for Type II ELMs on JET and AUG is consistent also

Understanding ELM size requires understanding transport processes



- ELM size shows a strong dependence on collisionality
 - Cause for concern on ITER
 - Must identify the origin of the collisionality scaling



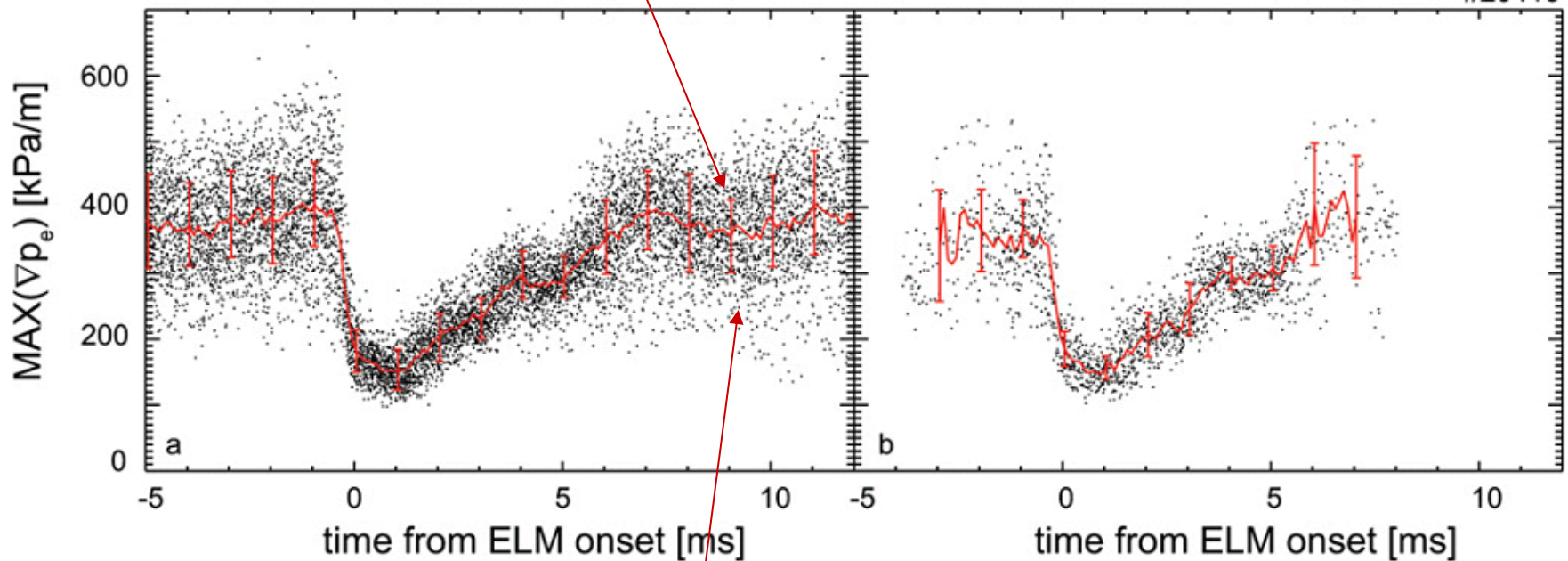
Loarte (PPCF 2003)

- Likely nonlinear physics

Behaviour of the pressure gradient

Saturated gradient, non-linear phase!

ASDEX Upgrade



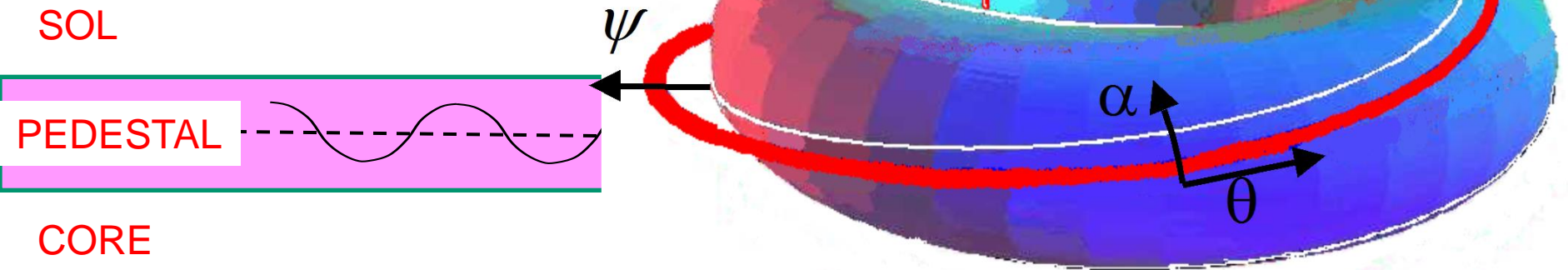
Burckhart, PPCF, 2010

Figure 7. ELM-synchronized maximal ∇p_e of (a) the slow and (b) the fast ELM cycles in discharge

Non-linear physics is important!

Nonlinear ballooning Theory

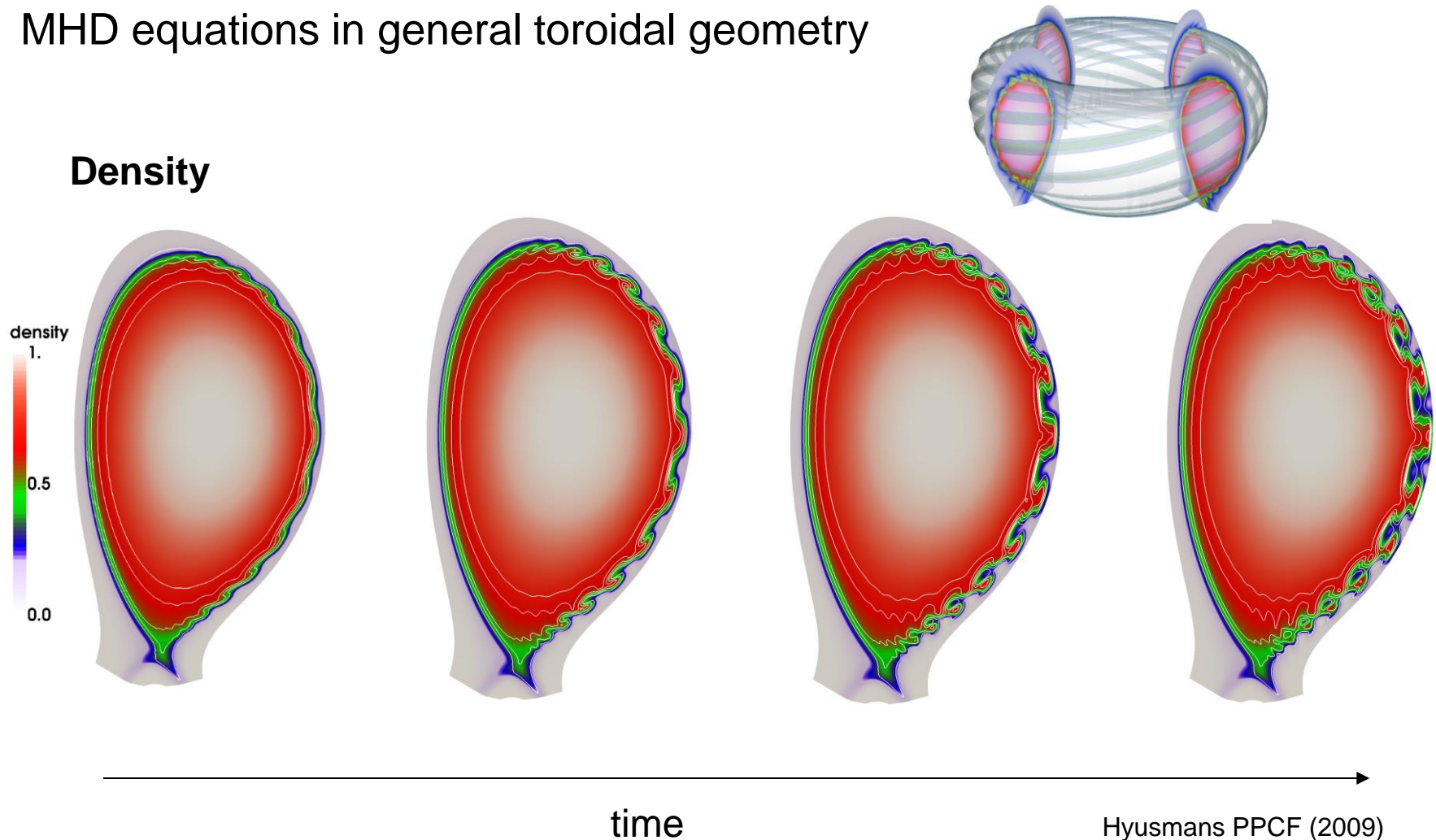
- Progress can be made analytically for the early nonlinear evolution (Wilson, Cowley PRL 2004)
- Predictions are
 - Initially sinusoidal mode narrows in direction across field lines, in flux surface
 - Mode tends to broaden radially, forming field-aligned filamentary structures
 - Even at linear marginal stability, as one enters nonlinear regime, mode suddenly erupts
 - Maximum displacement (field line), elongated along



- Filament could strike material surface on outboard side while remaining connected to pedestal on inboard
 - Potential damage to plasma-facing components, especially on ITER

Non-linear simulations of ELMs

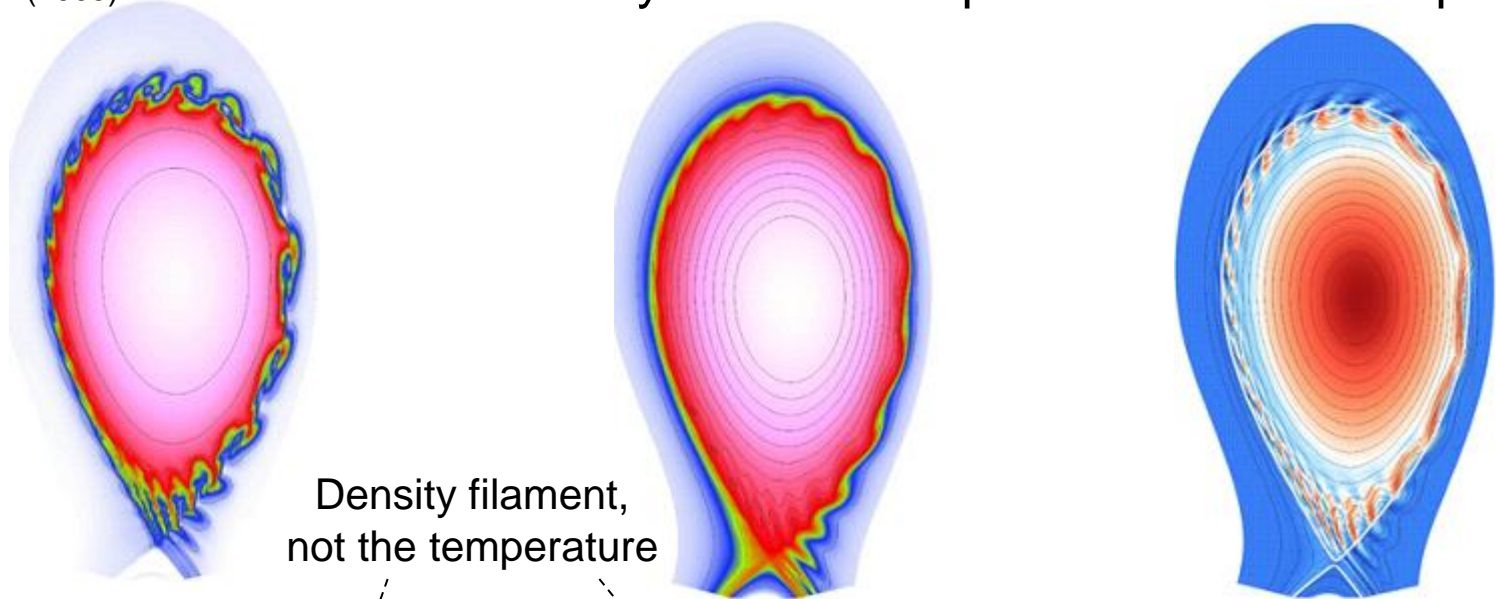
Non-linear MHD code JOREK solves the time evolution of the reduced MHD equations in general toroidal geometry



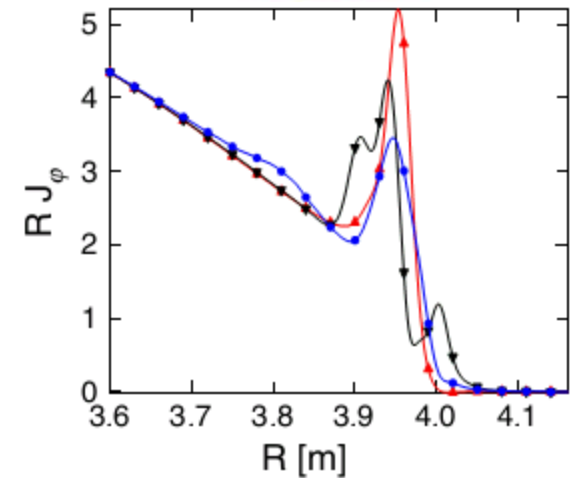
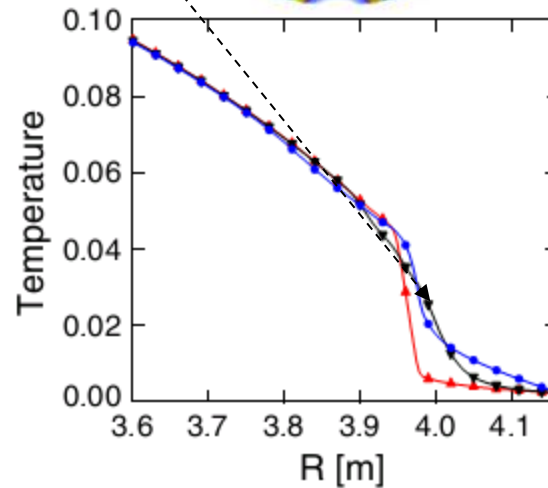
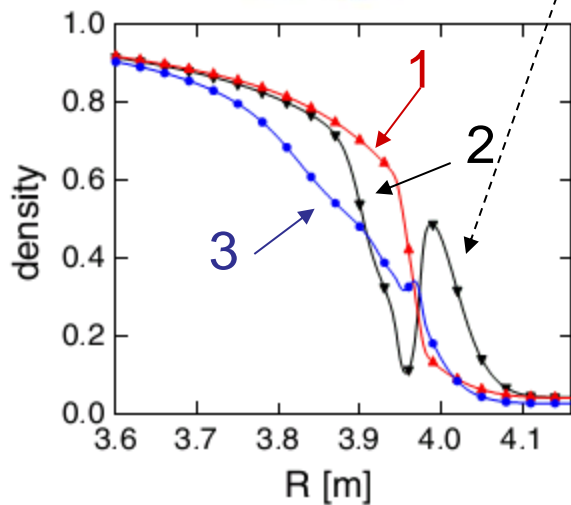
Non-linear simulations of ELMs

Hyusmans PPCF (2009)

Formation of density filaments expelled across the separatrix.



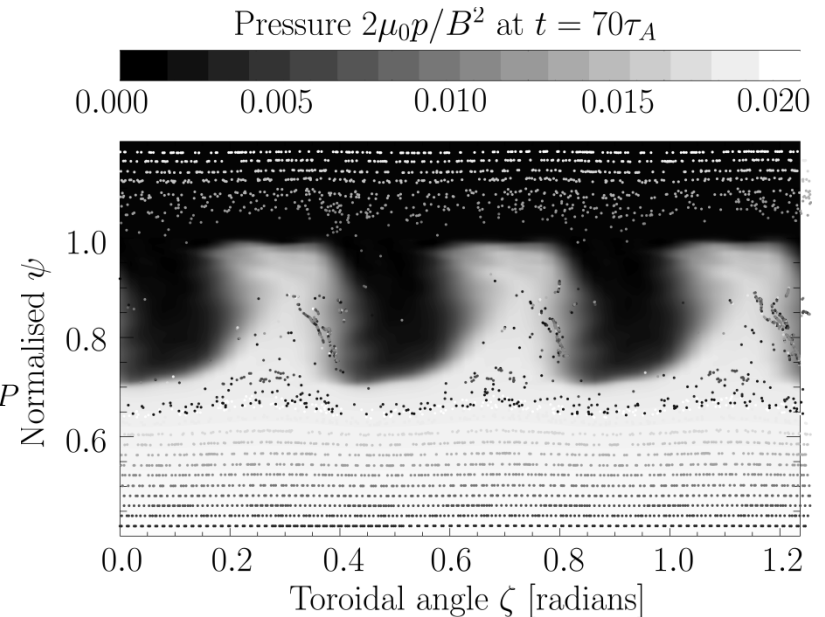
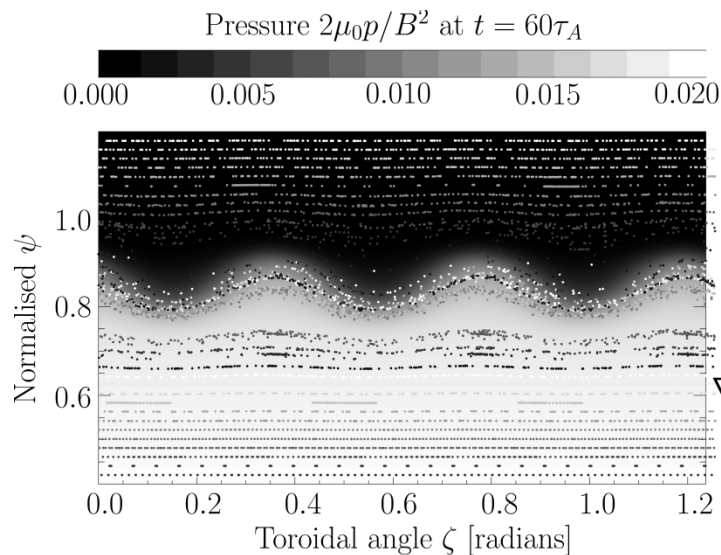
Density filament,
not the temperature



Nonlinear MHD modelling: Transport processes

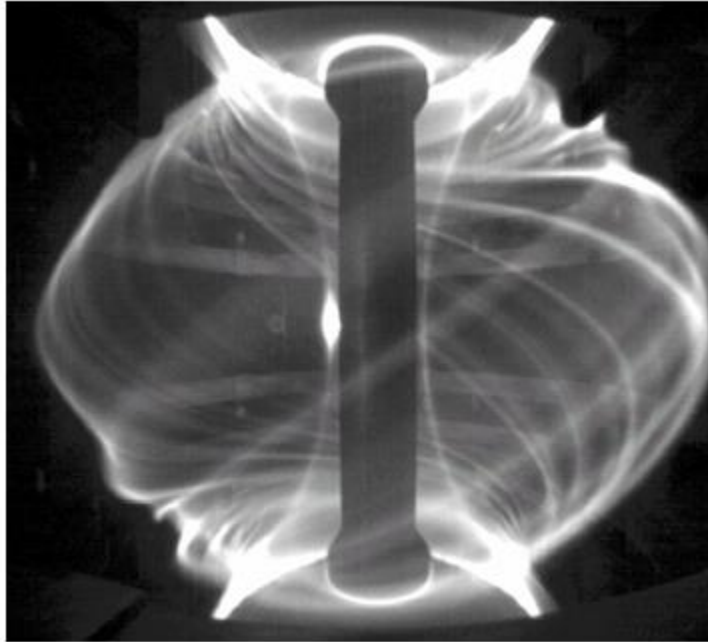


- Nonlinear MHD codes can probe the transport processes during the ELM
 - JOREK: electron heat transport dominated by parallel conductivity; density is convected into SOL; ion heat is a mixture
 - BOUT++ and JOREK observe stochastic magnetic field at the edge, which seems to play a role in the transport



Xu, Dudson, et al, PRL 2010

ELM Filament Observations. Fast cameras (eg MAST)

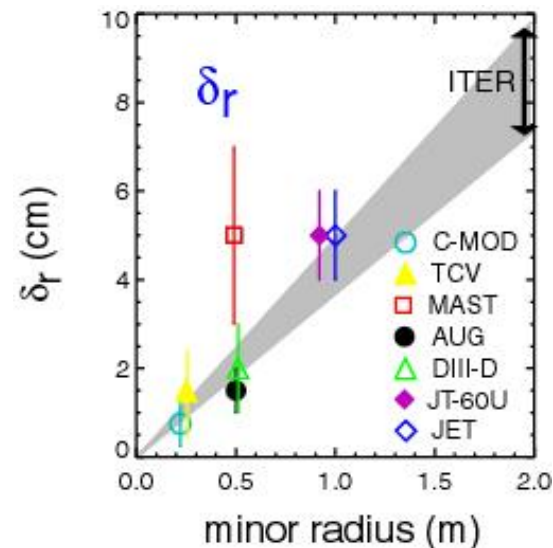
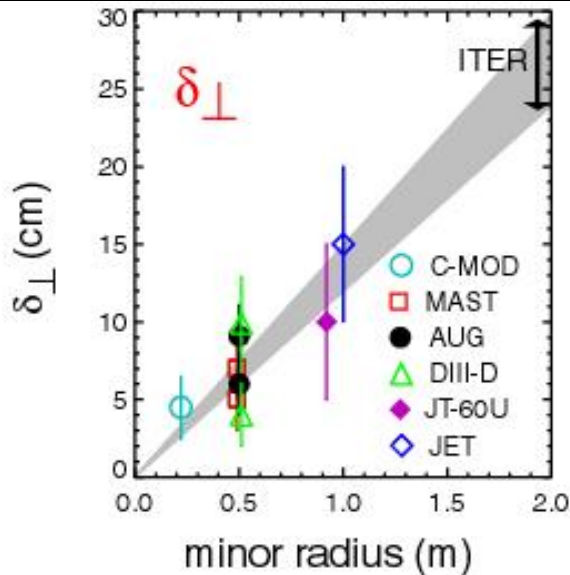


High-speed video image of the MAST plasma obtained at the start of an ELM



The predicted structure of an ELM in the MAST tokamak plasma geometry, based on the nonlinear ballooning mode theory

ELM Filament Observations



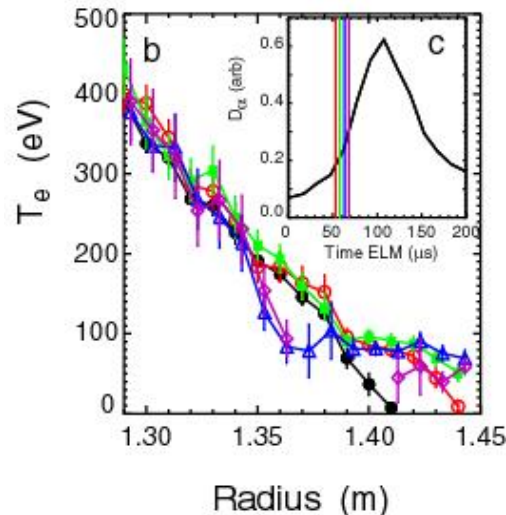
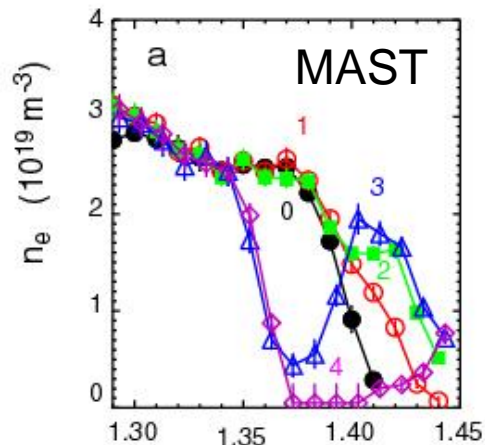
A Kirk JNM 2009

- Fast cameras provide the most direct observation of filaments
- They twist to align with magnetic field lines as they erupt
- One can measure their ejection velocity: clear acceleration on MAST, but constant velocity on AUG
- Filaments scale with machine size, and are oval: \perp extent more in flux surface than radial

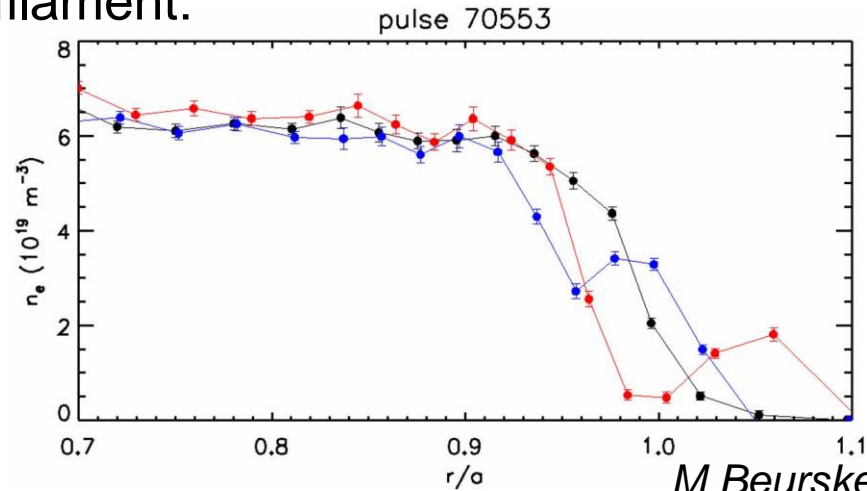
ELM filament observation: Thomson scattering



- TS measurements of filaments on MAST and JET provide a measure of the thermal energy stored in a filament:



A Kirk, PRL 2006



JET

M Beurskens, PPCF 2007

- Assuming $T_i = T_e$, stored energy in filament $\sim 2.5\%$ ELM energy loss
- 10 filaments only account for $\sim 25\%$ of the loss
- Another mechanism operates (filament syphoning energy from pedestal, or something else?)

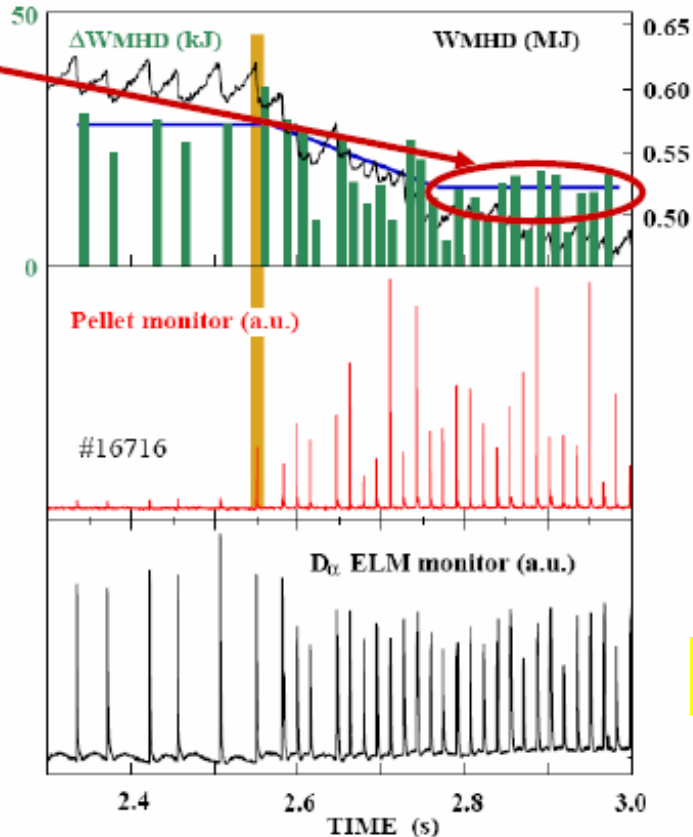
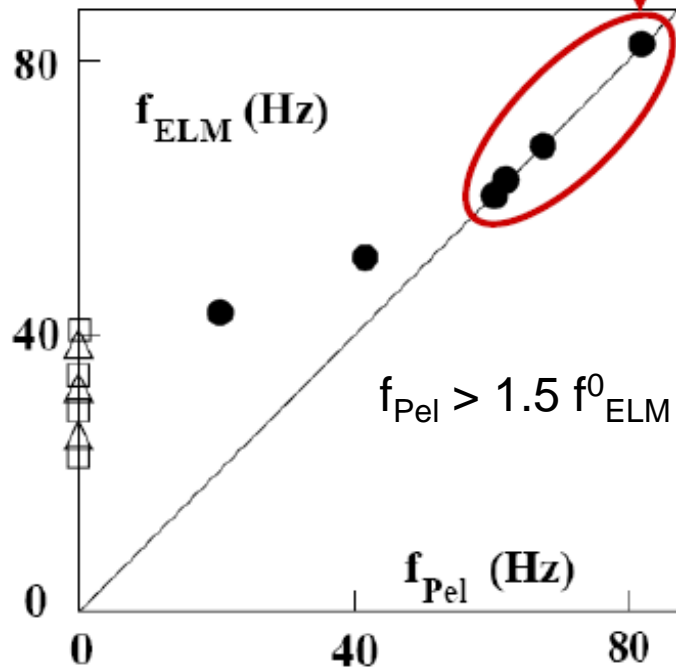
Control of ELMs

ELM size reduction by pellet injection

Type-I ELM frequency can be increased by injection of small deuterium pellets, provided that pellet freq. > 1.5 natural ELM freq. (results from AUG)

Can the effects of plasma fuelling and ELM pacing be decoupled?

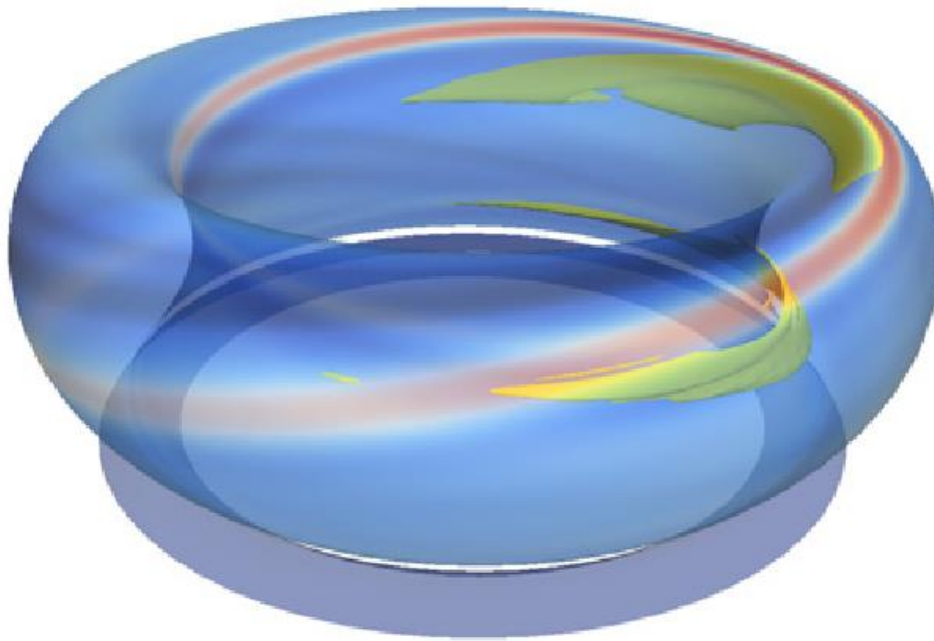
Only here we have **suitable pacing**, elsewhere it is just triggering



P T Lang, et al., Plasma Phys. Control. Fusion 46 (2004) L31–L39

AUG

JOEK

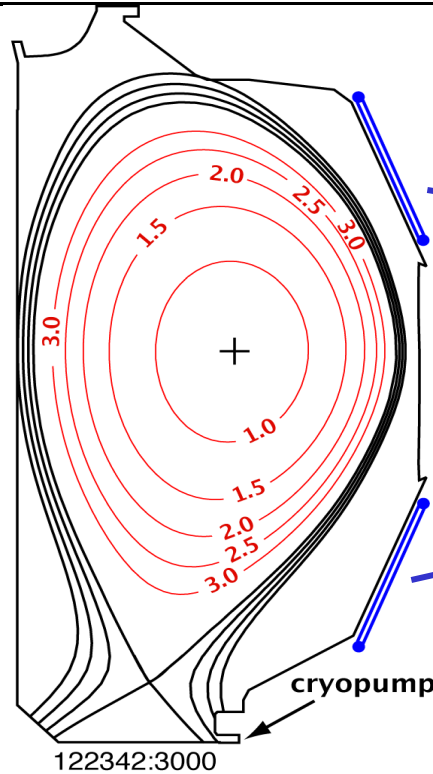


G T A Huysmans, PPCF 51 (2009)

- A strong pressure develops in the high density plasmoid, in this case the maximum pressure is approx. 5 times the pressure on axis.
- There is a strong initial growth of the low- n modes followed by a growth phase of the higher- n modes ballooning like modes.
- The coupled toroidal harmonics lead to one single helical perturbation centred on the field line of the original pellet position.

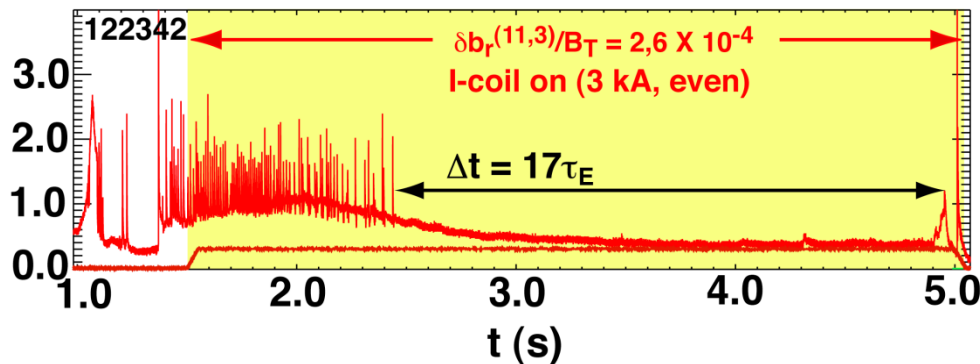
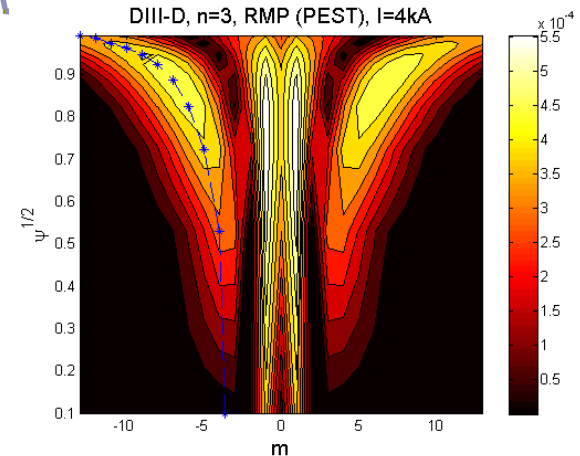
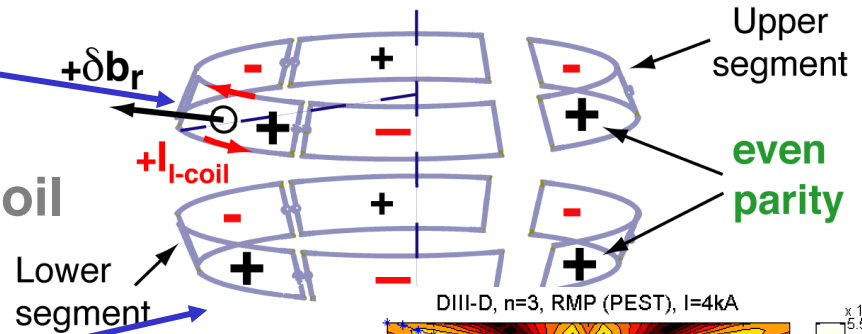
Simulations of pellets injected in the H-mode pedestal show that pellet perturbation can drive the plasma unstable to ballooning modes.

Experiments of Active Control of ELMs with a RMP on DIII-D Tokamak



Internal coil
(I-coil)

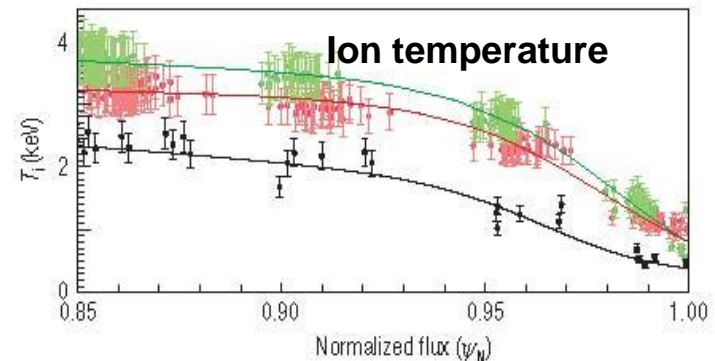
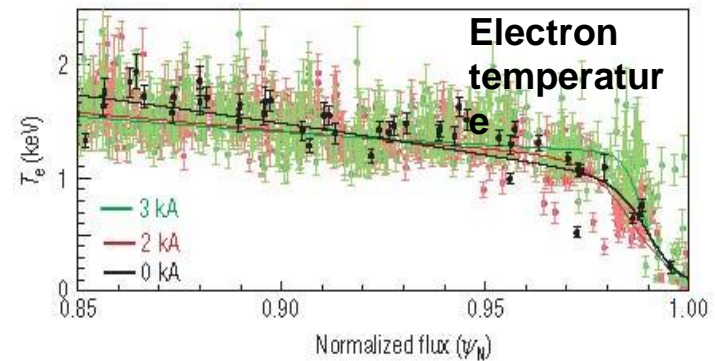
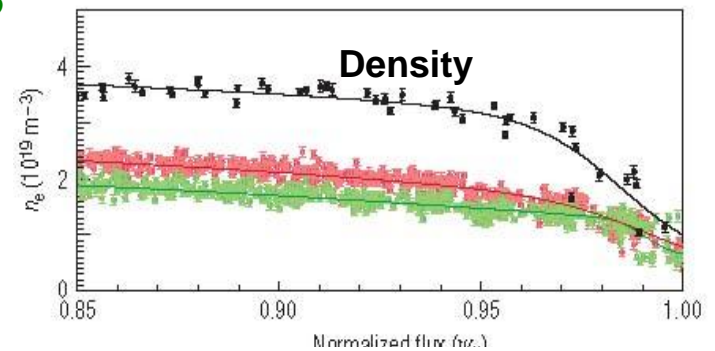
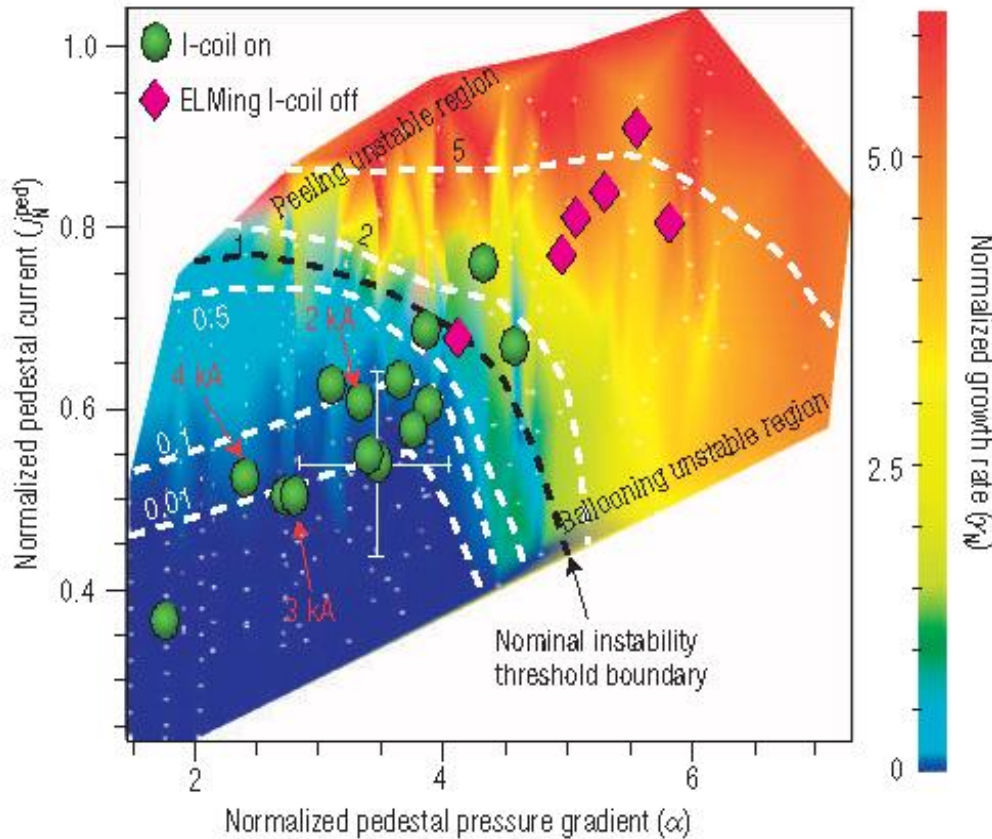
**n=3 I-coil configuration
(strong RMP - even parity)**



T. E. Evans, et al., PRL, 92, 235003 (2004)
T. E. Evans, et al., Nature physics, Vol. 2, p419, June 2006
T. E. Evans, et al., Phys. Plasmas 13, 056121 (2006).

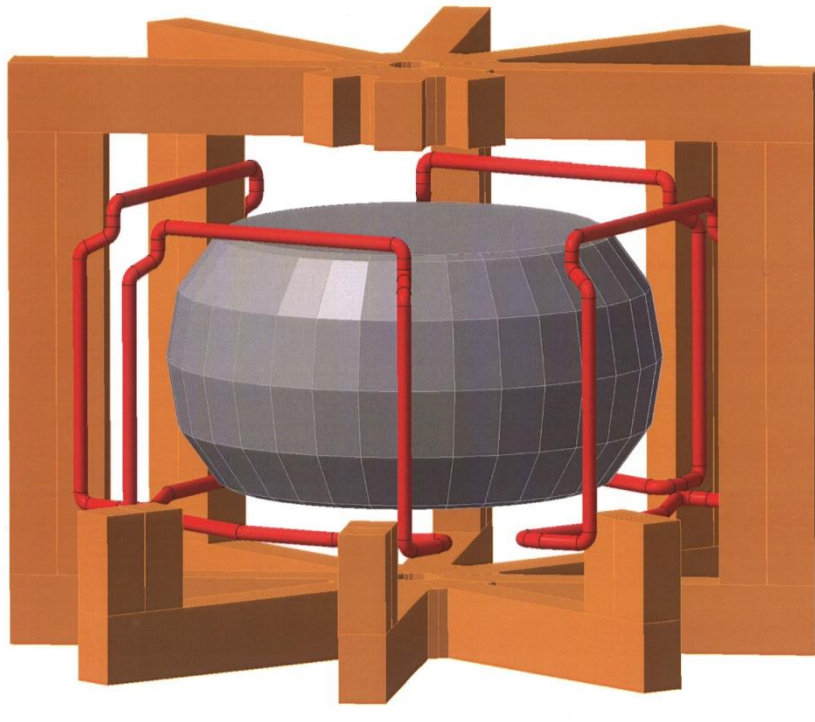
Dominant mechanism of ELM suppression

T. E. Evans, et al., Nature physics, Vol. 2, p419, June 2006



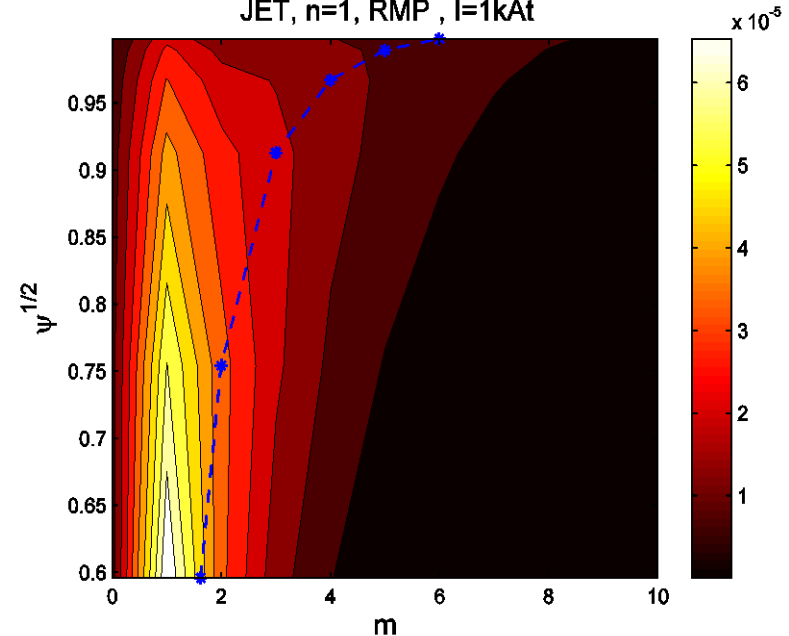
Reduction of edge pressure below instability threshold

Error field correct coils (EFCC) on JET



$$I_{\text{EFCC}} = 1 \text{ kAt}; B_t = 1.84 \text{ T}$$

JET, $n=1$, RMP, $I=1\text{kAt}$



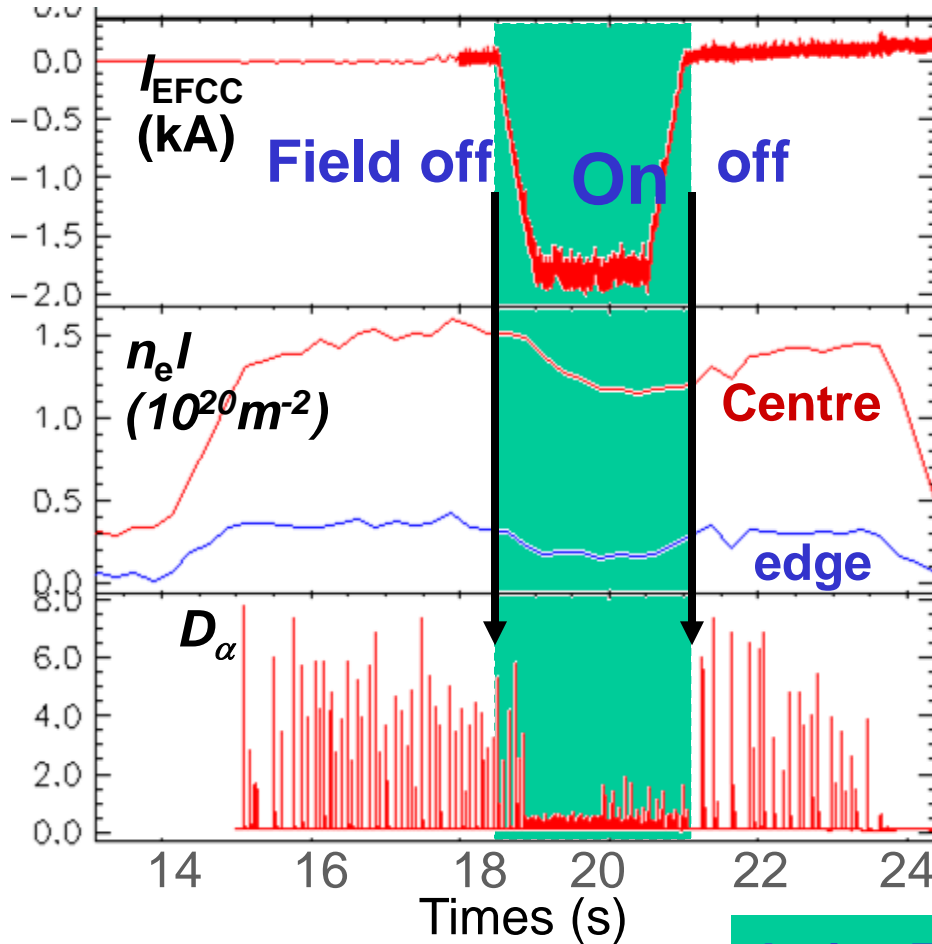
- Depending on the relative phasing of the currents in individual coils, either $n=1$ or $n=2$ fields can be generated
- $I_{\text{Coil}} \leq 3 \text{ kA} \times 16 \text{ turns}$ ($n = 1$ and 2)
- $R \sim 6 \text{ m}$; Size $\sim 6 \text{ m} \times 6 \text{ m}$
- B_t at wall $\sim 0.25 \text{ mT/kAt}$

Y.Liang et al., PPCF 2007

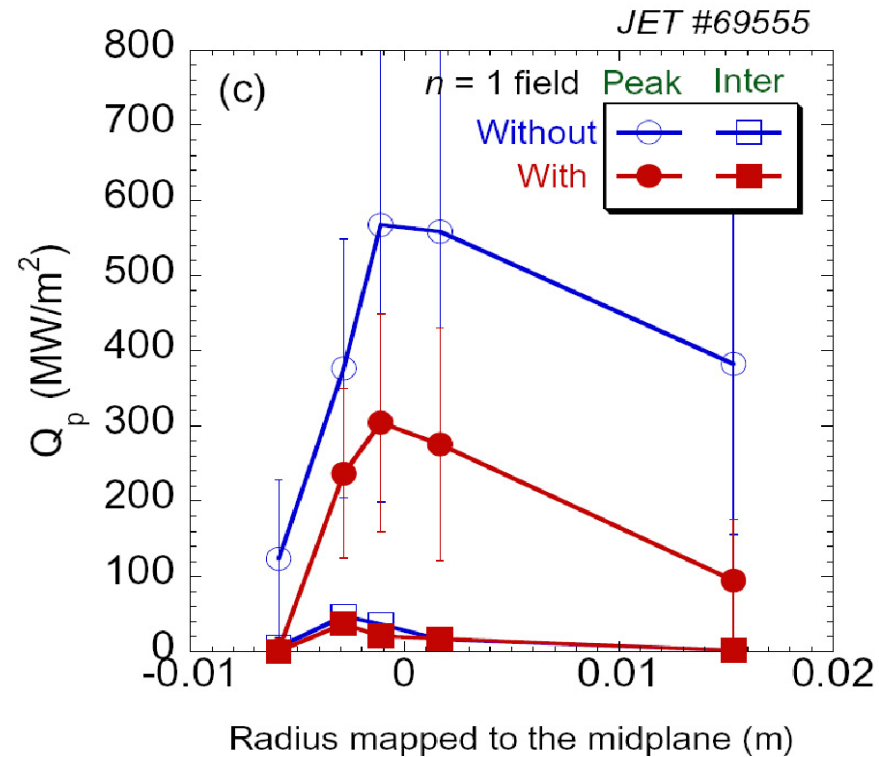
Active ELM control with $n = 1$ magnetic perturbation field on JET



$I_p = 1.8$ MA; $B_t = 2.1$ T; $q_{95} \sim 4.0$; $\delta_U \sim 0.45$ JET#69557



Heat flux onto the outer divertor



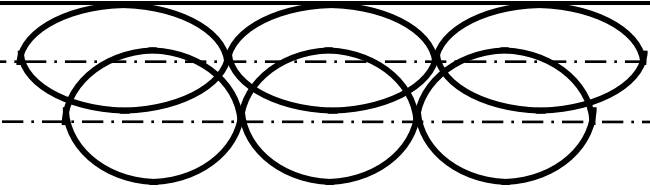
Y Liang, et al, PRL, 98, 265004 (2007)
 Y Liang, et al, PPCF, 49, B581 (2007)
 Y Liang et al, JNM, 390–391, 733–739 (2009)

Active ELM control (frequency/size) observed in a wide q_{95} window, but no ELM suppression

Equilibrium Magnetic Field at Plasma Edge

$$q = m/n$$

$$q = (m+1)/n$$

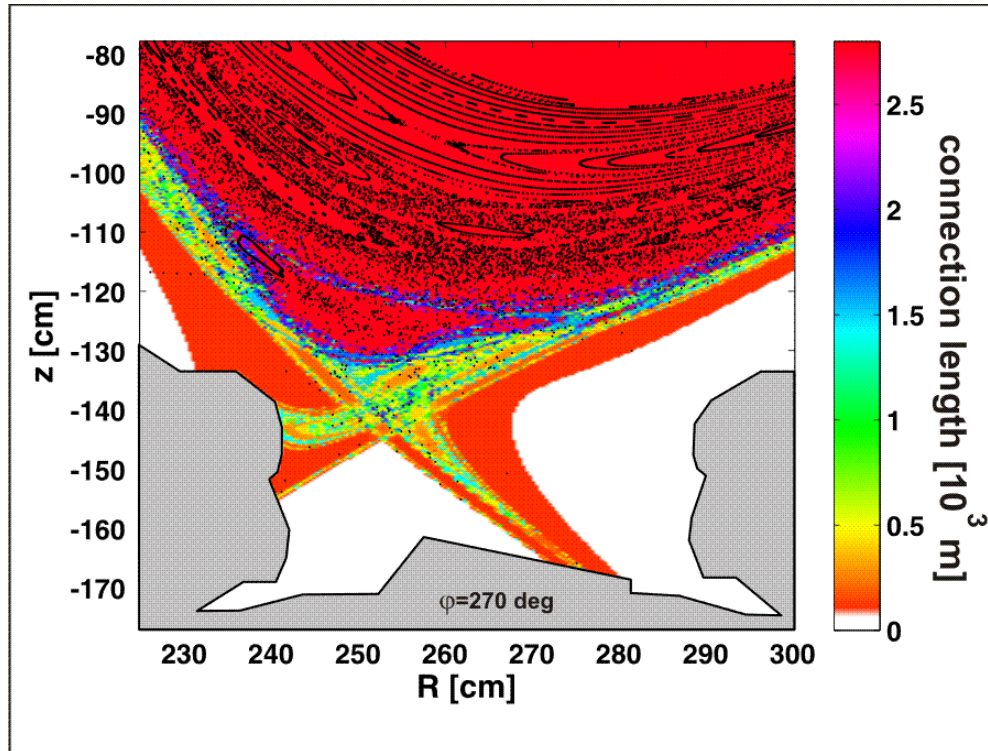


Chirikov parameter

$$\sigma_{m,m+1} = \frac{W_{n,m} + W_{n,m+1}}{2\delta_{m,m+1}}$$

larger than 1

- Splitting of strike point
- Spin-up plasma rotation to co-current direction

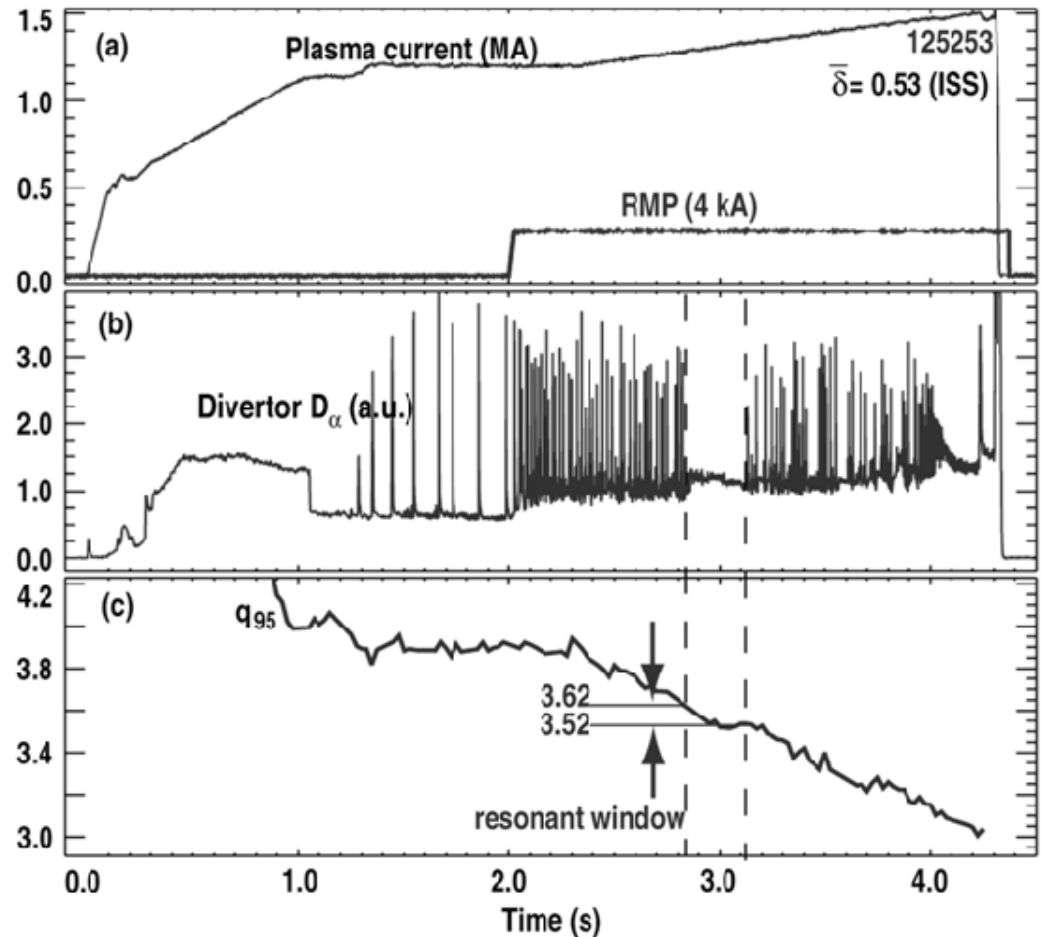


Edge Ergodisation with a magnetic perturbation

ELM suppression window on DIII-D

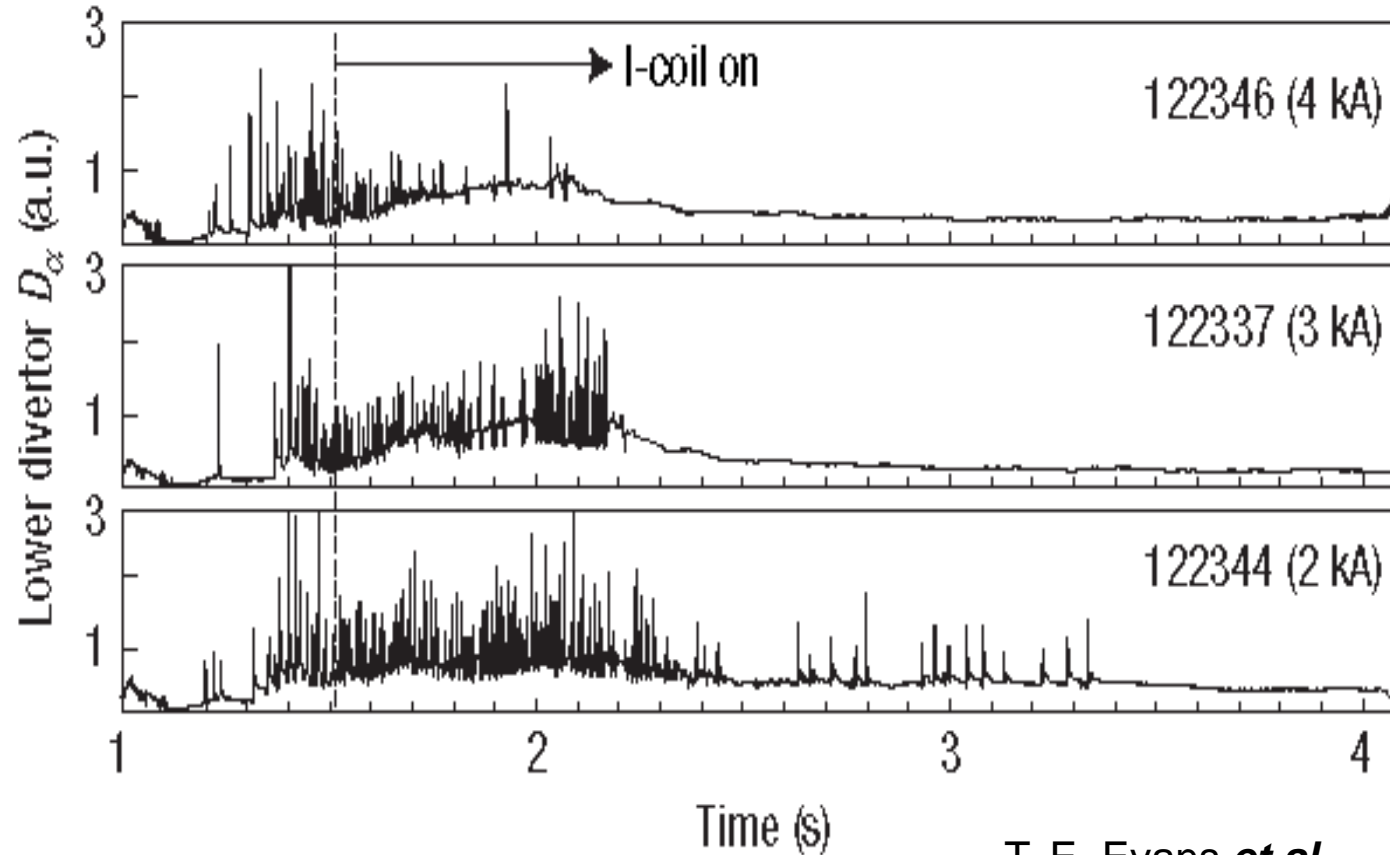


- ✓ ELM suppression achieved in a narrow q_{95} window on DIII-D with an $n=3$ field induced by the I-coils.
- ✓ q_{95} ELM suppression window can be enlarged slightly with a mixed $n=1$ and $n=3$ fields.



T.E. Evans, et al.,
NF 48 (2008) 024002

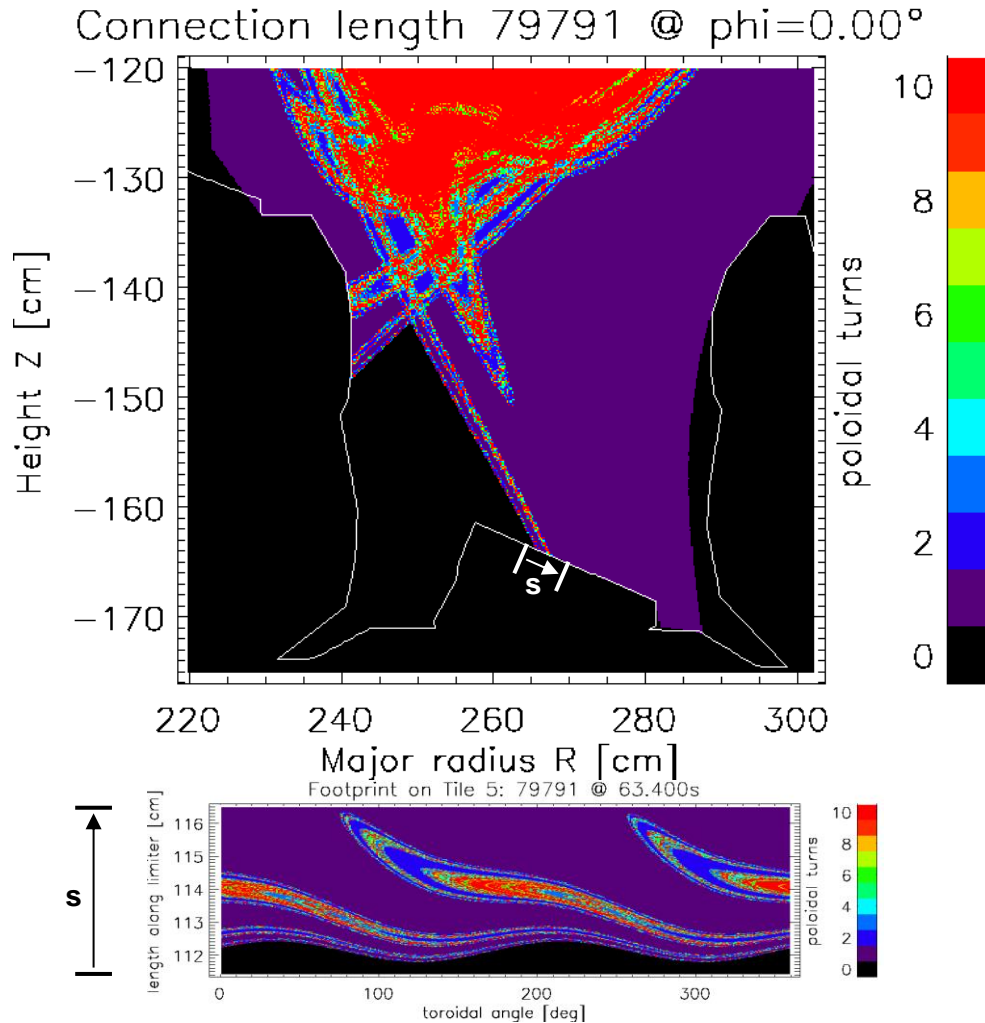
Threshold of ELM suppression



There is a threshold of ELM suppression in the amplitude of the $n = 3$ field.

T. E. Evans *et al*
Nature Physics 2 (2006) 419

Toroidal evolution of strike point



- Field line tracing in vacuum approximation (superposition of equilibrium and perturbation field)
- No screening of RMP by poloidal rotation
- Ergodic field lines form lobes which generate multiple strike points on the divertor
- Strike point splitting depends on toroidal position
- Footprint represents $N=2$ symmetry of perturbation field

D. Harting, JET science meeting 2010



O. Schmitz, PPCF (2008)

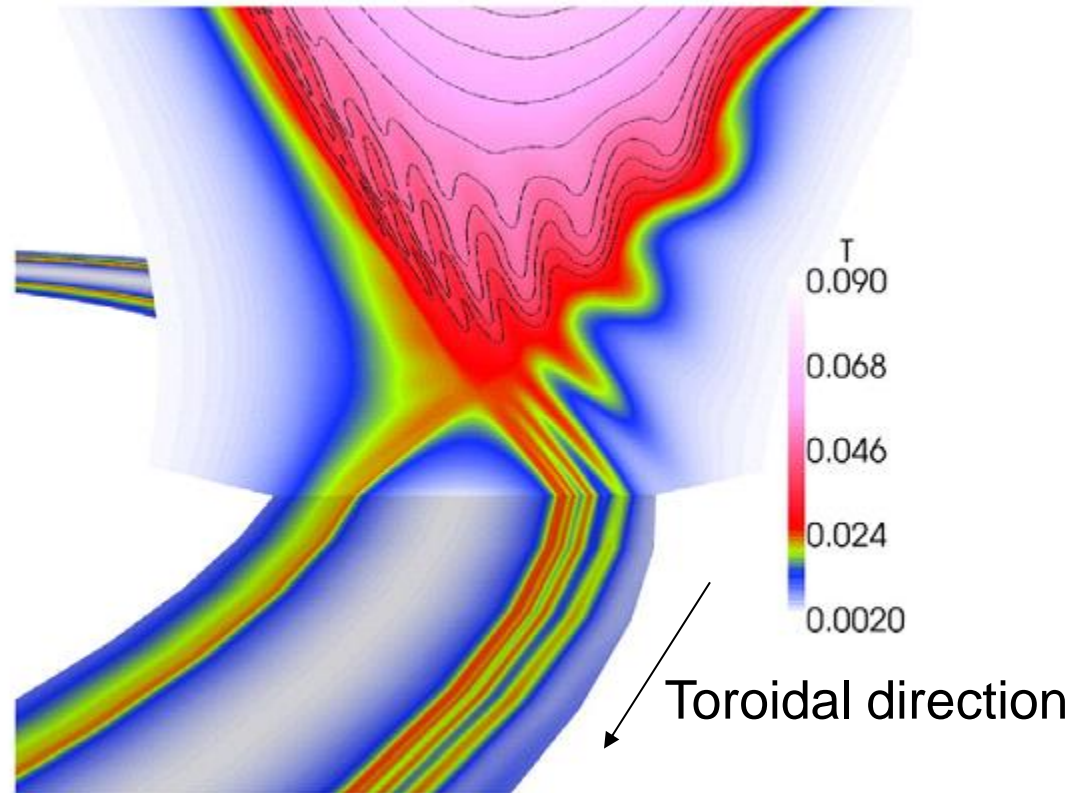
I. Joseph JNM, 2007

Splitting of the inner strike-point has been observed during ELM suppression with an $n = 3$ field on DIII-D.

Nonlinear simulations of ELMs



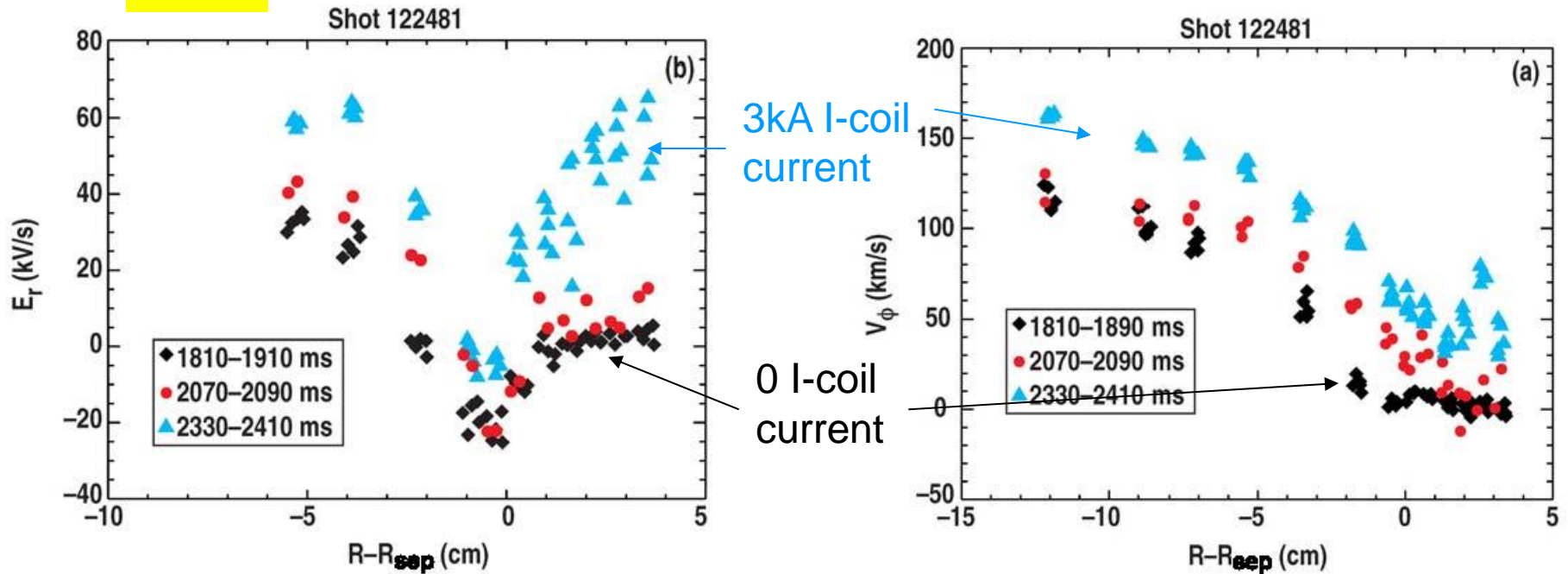
Hyusmans PPCF (2009)



A poloidal and toroidal cut of the plasma temperature

Influence of magnetic perturbation on the Edge Electric field and rotation

DIII-D



With an $n = 3$ field applied,

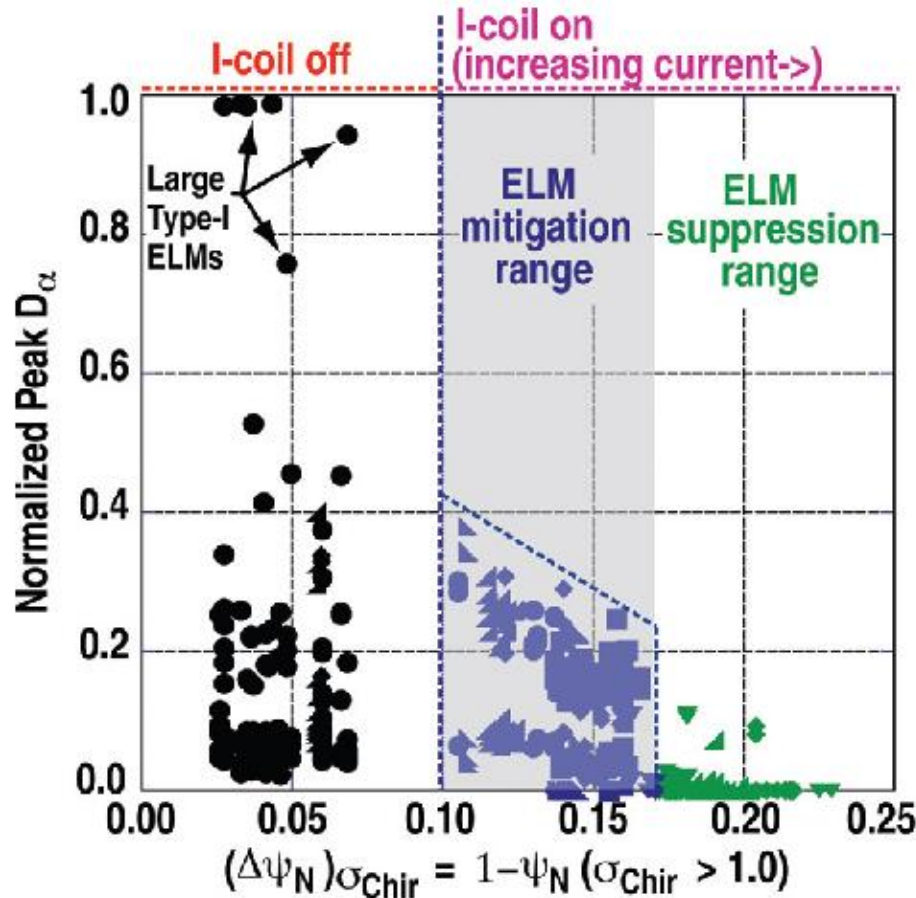
edge $E_r \rightarrow$ more positive;

spin-up plasma rotation in co-current direction,

A large enhancement of the electron losses rather than ions by reason of the **edge ergodisation**.

K. Burrell, PPCF 47, B37, 2005

Criterion for ELM suppression with RMPs



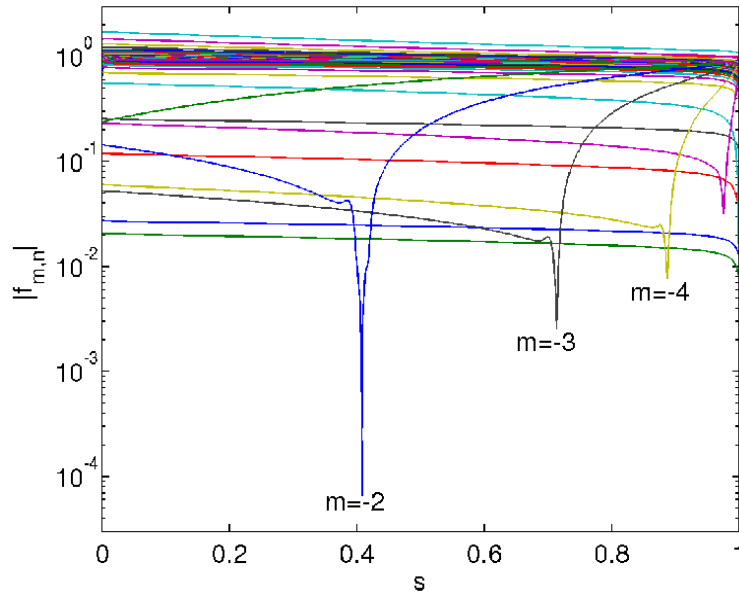
M.J. Schaffer, et al.,
IEEE (2009); NF (2008)

✓ Chirikov parameter number larger than 1 in the edge layer ($\sqrt{\psi} > 0.925$).

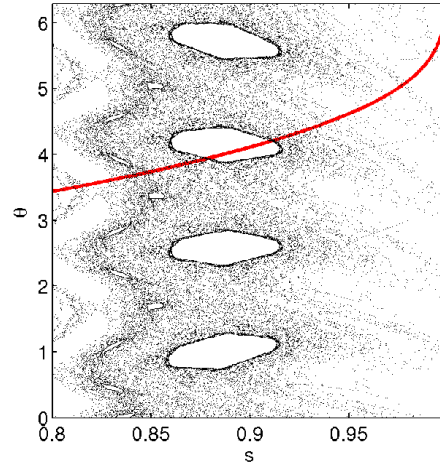
Effect of plasma shielding of the RMP

M. Heyn, JET science meeting, 2010

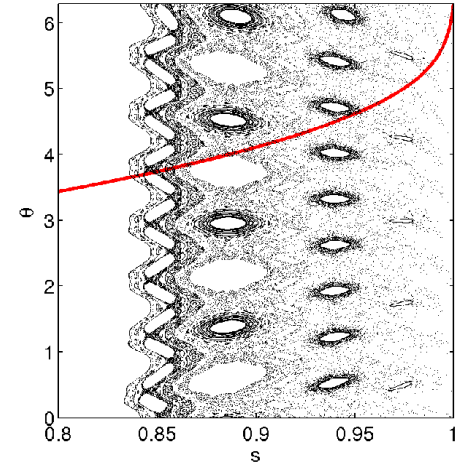
$$f_{mn} = B_{r,mn}^{(\text{plas})} / B_{r,mn}^{(\text{vac})}$$



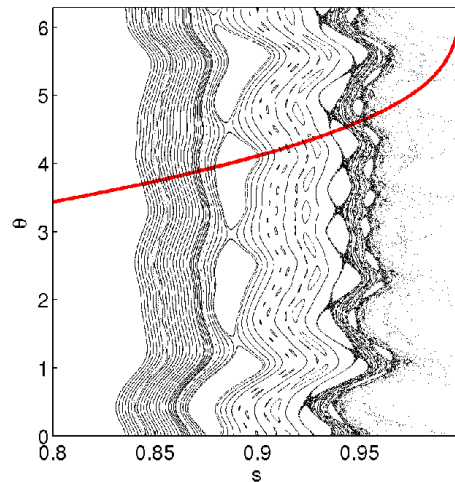
✓ The resonant perturbation is shielded due to plasma rotation and the magnetic field topology in the plasma core is not affected by RMP's.



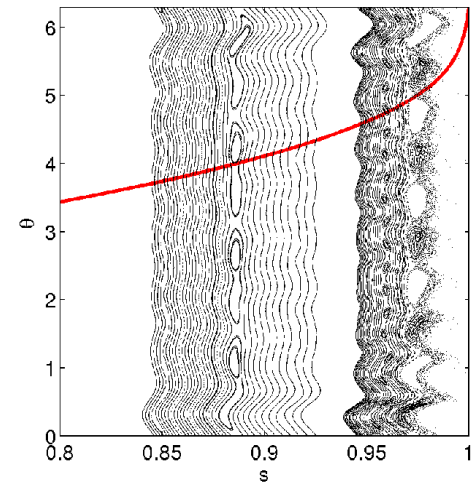
vacuum, $n = 1$



vacuum, $n = 2$

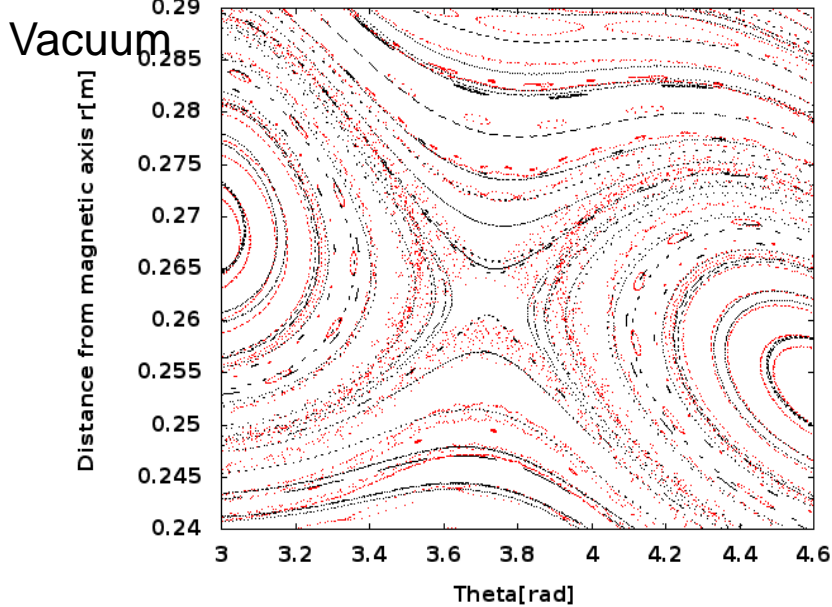


plasma, $n = 1$



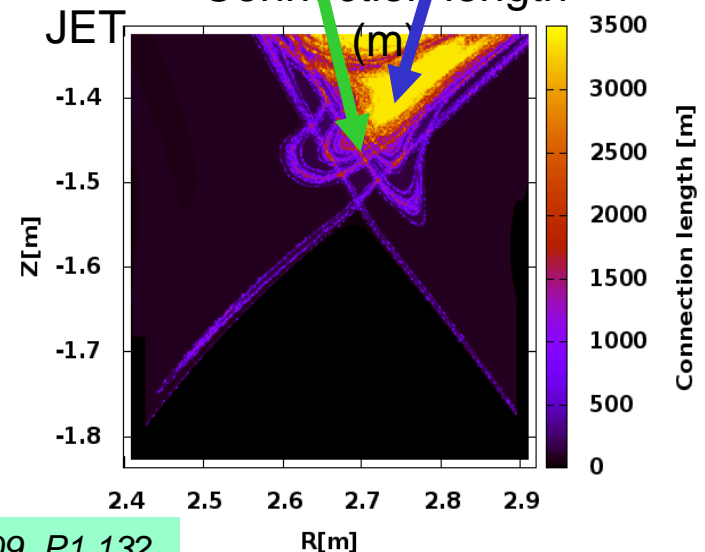
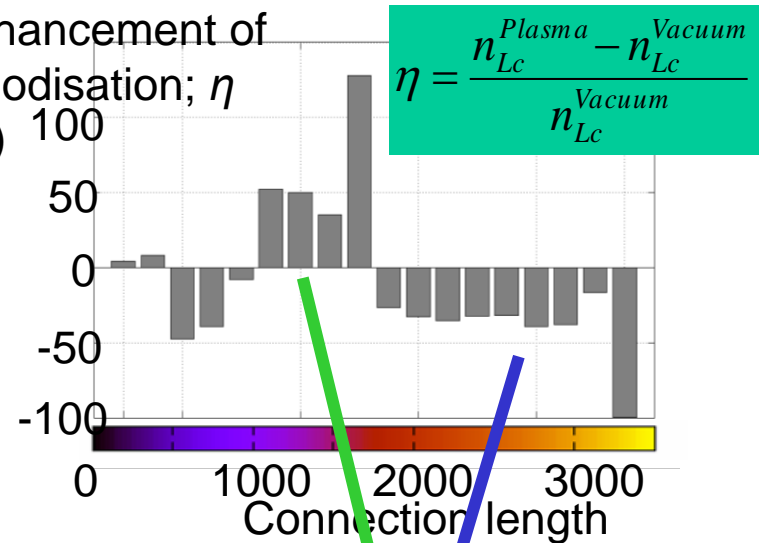
plasma, $n = 2$

3-D Equilibrium calculation by HINT2 Code



- Flattening of j and p at the islands leads to an ergodisation at the island X-points
- Strong enhancement of ergodisation at the X-point region due to plasma response may explain the density pump-out seen already at a small amplitude of the perturbation field

Enhancement of ergodisation; η (%)



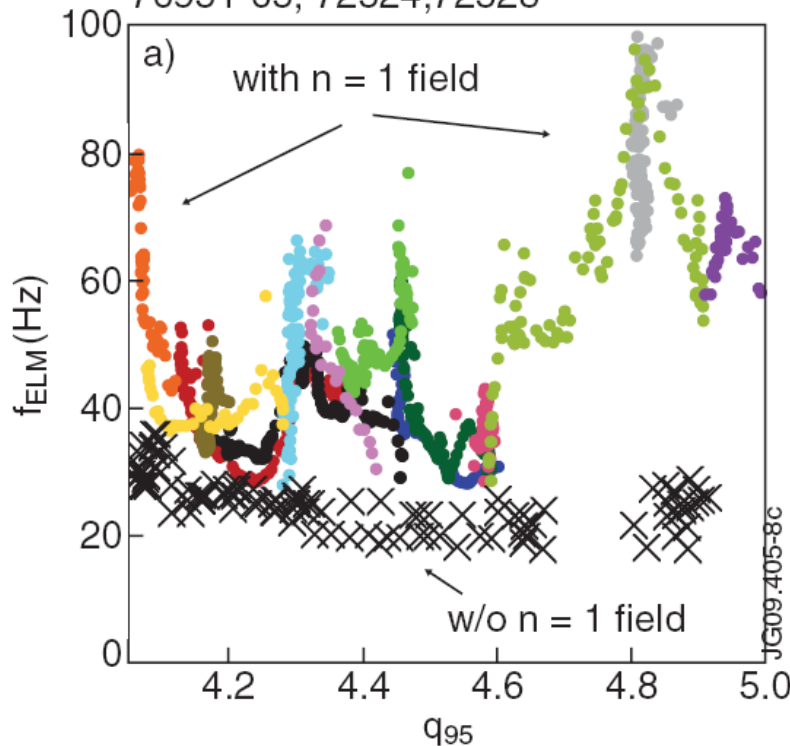
C. Wiegmann, et al, EPS2009, P1.132

Observations of Multi-Resonance Effect in ELM Control with Perturbation Fields on the JET



JET Pulse No's:
76951-65; 72524,72528

Y. Liang et al., PRL 105, 065001 (2010)



A model in which the ELM width is determined by a localized relaxation to a profile which is stable to peeling modes can qualitatively predict this multi-resonance effect with a low n field. The dominant unstable peeling mode number and ELM frequency depends on the amplitude of the normalized edge currents as well as q_{95} .

- Multiple resonances in f_{ELM} vs q_{95} have been observed with $n = 1$ and 2 fields
- The mechanism of edge ergodisation, can not explain the multi-resonance effect observed with the low n fields on JET.
- Possible explanation in terms of ideal peeling mode model by *Gimblett, PRL, 2006*.

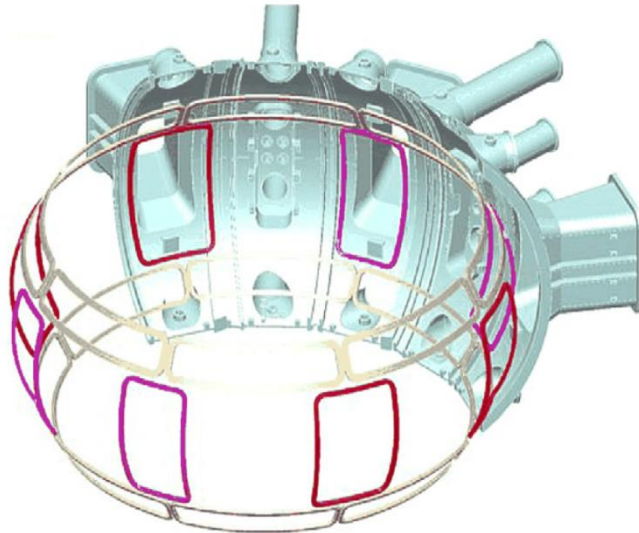
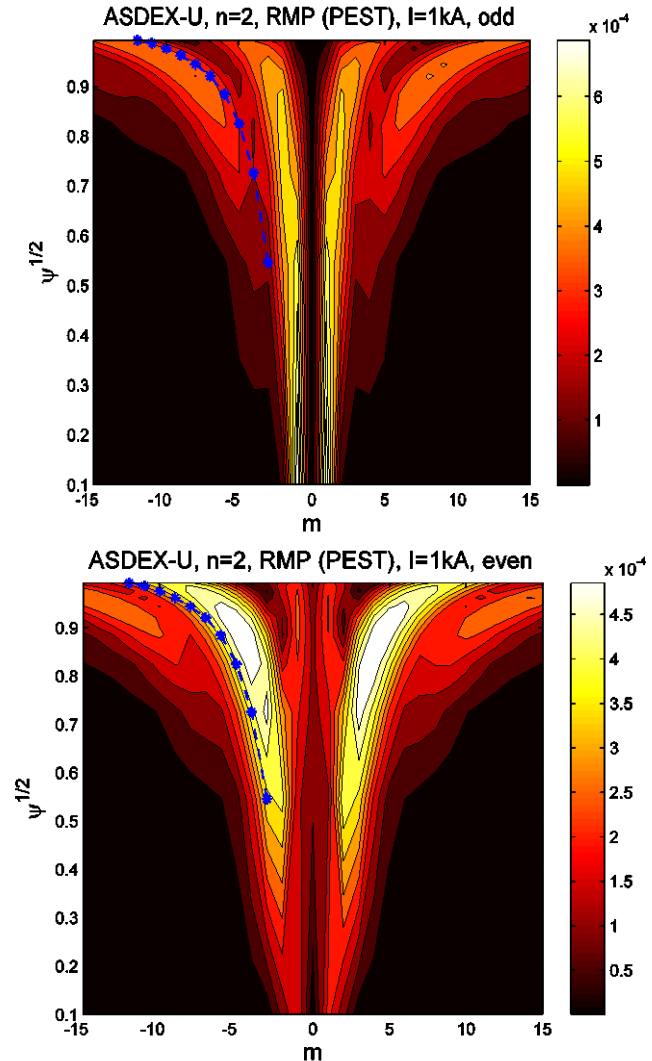


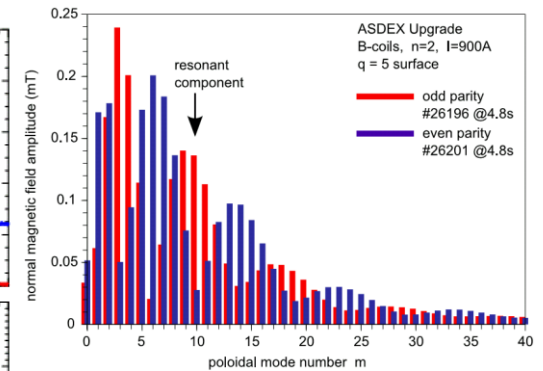
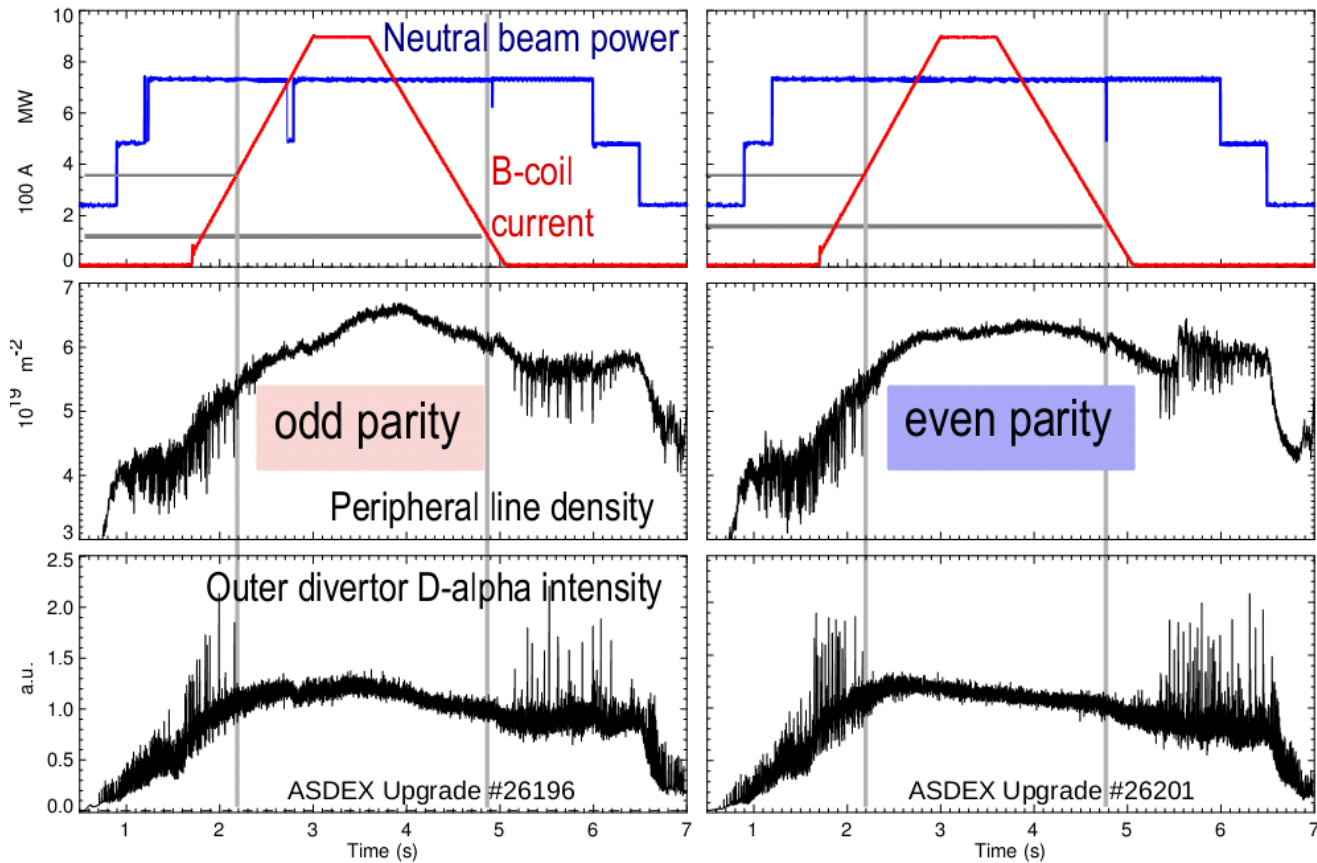
Fig. 1. 3D view of active in-vessel coils.

**W Suttrop, Fusion
Engineering and Design 84
(2009) 290**

In 2011: Two rows $\times 4$ toroidally distributed coils ($n = 2$).
Single DC supply (all coils in series / anti-series).



ELM mitigation on AUG

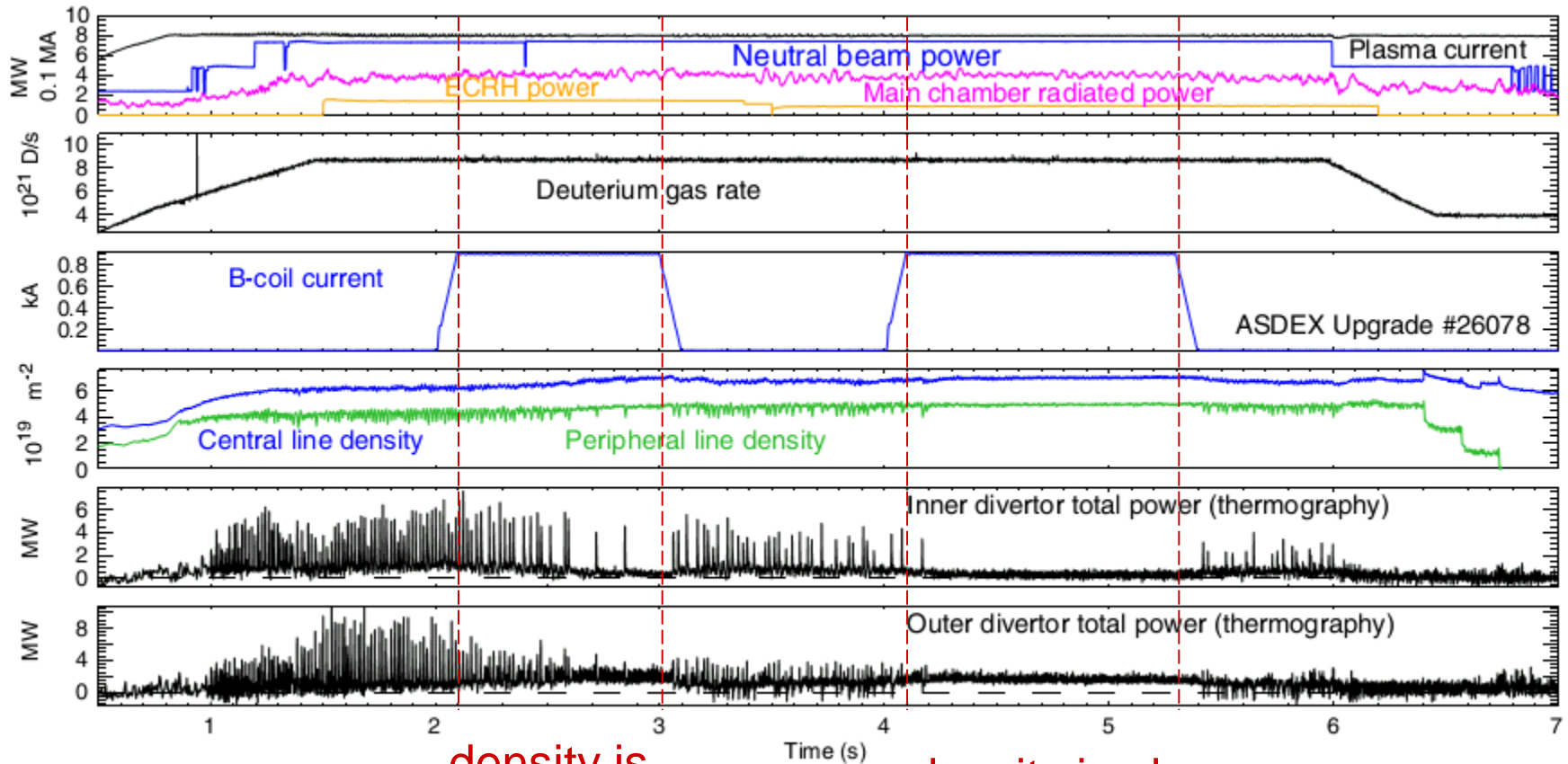


Resonant and non-resonant variants work in the same way!
... which is in contradiction to stochastic hypothesis...

Hysteresis: $I_{\text{coil}} = 350 \text{ A}$ to and $\approx 150 \text{ A}$ from ELM-mitigated state

W Suttrop, PRL (2010)

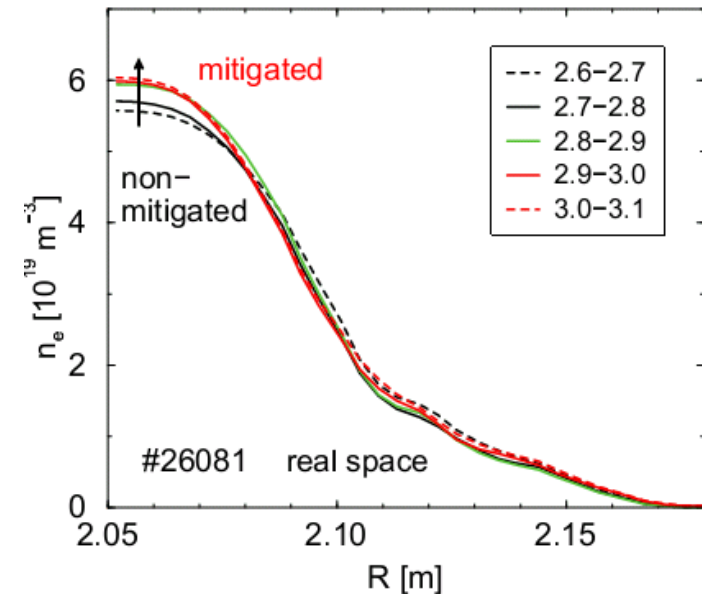
ELM mitigation on AUG



density is
around the
threshold

density is above
the threshold
(mitigation)

- Type-I ELMs replaced by frequent small ELMs (not a gradual evolution of ELM losses)
- Particle confinement, pedestal density increase (no “pump-out”)
- Energy confinement (stored energy) \approx unchanged
W concentration, Z_{eff} not increased
- Minimum density for ELM mitigation
Empirical “scaling”: $n_{\text{edge.min}} = 0.65 n_{\text{GW}}$
Universal? Physical meaning?
- ELM mitigation apparently insensitive to resonance condition
Demonstrated at $q_{95} = 5.5$, but true for all q ?



DIII-D $n = 3$, I-coils

- ELM suppression in a narrow range of q_{95}
- ELM mitigation in a wide range of q_{95}

JET $n = 1, 2$ EFCC

→ ELM mitigation

global effect in a wide range of q_{95}

multi-resonance effect in multiple narrow q_{95} windows

MAST $n = 1, 2$ EFCC; $n=3$ I-coils

→ ELM mitigation (q_{95} dependence)

AUG $n = 2$ B-coils

- ELM mitigation in a relative wide range of q_{95}
- Thresholds for RMP ELM mitigation

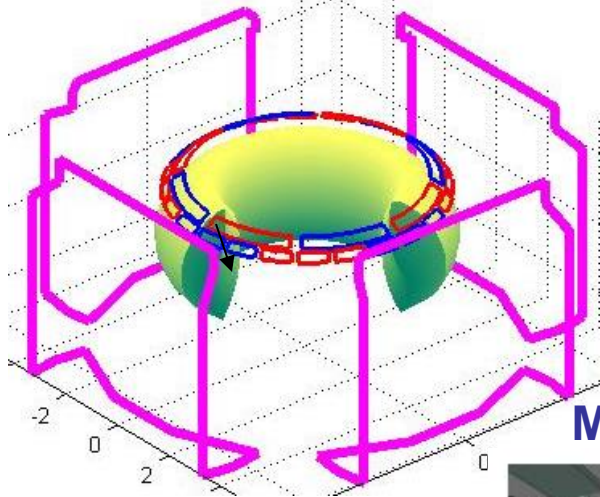
- Is the amplitude of the effective RMP important? → **Yes**
 - Plasma Rotational screening effect
 - Field penetration → **Yes, but how deep the RMP field have to penetrate into a plasma for ELM suppression?**

- Is the target plasma itself important? → **Yes**
 - Operation regime (ELM stability) → **Unknown**
 - Plasma shaping (ELM stability) → not very important
 - Collisionality (depending on the device; → **Unknown**)
 - q_{95} → **Yes**
 - Beta dependence? (→ **DIII-D Yes**)

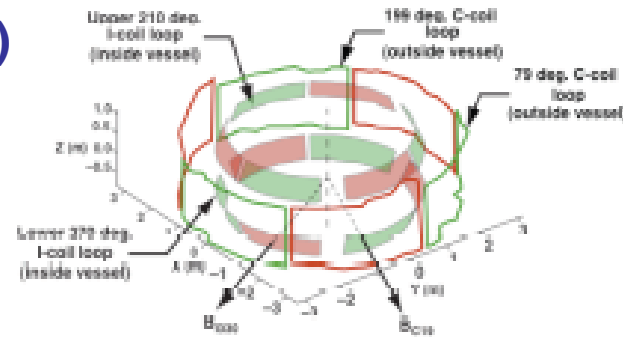
RMP ELM control Experiments



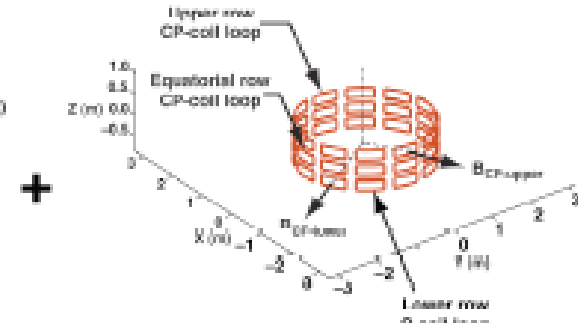
JET EFCC & In-vessel coils (planned)



DIII-D existing

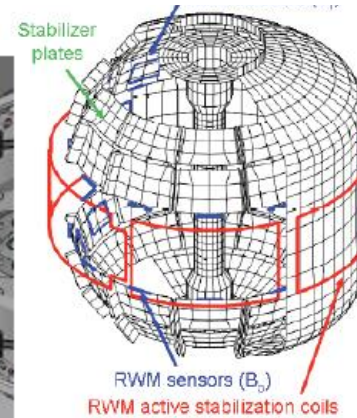
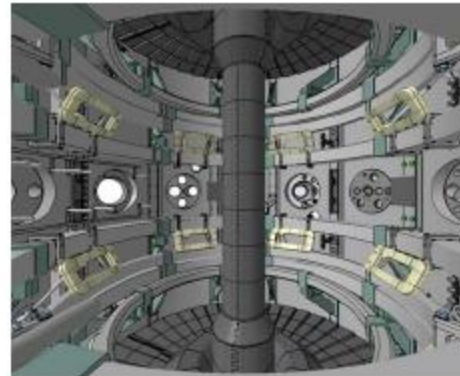


DIII-D planned



MAST

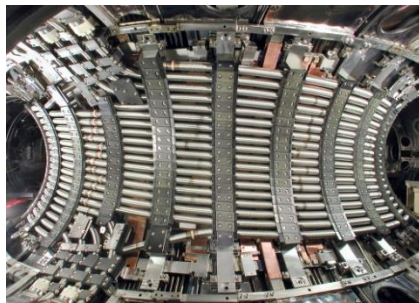
NSTX



ASDEX-U



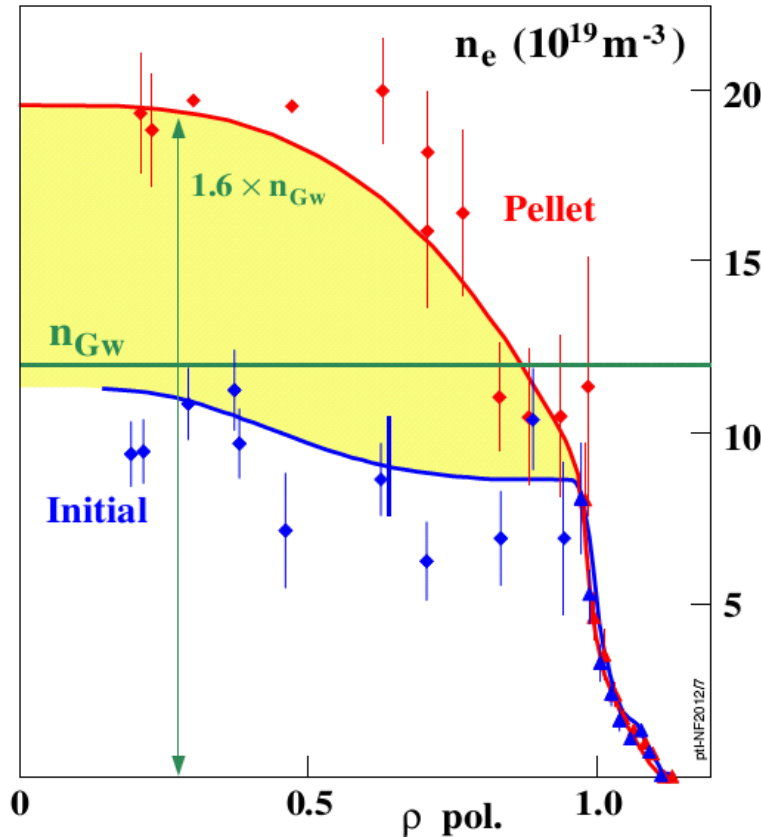
TEXTOR



+ EAST

..... providing input to modelling for ITER.

ASDEX Upgrade



External coils + pellets

Central density could be increased up to $n \approx 1.6n_G$

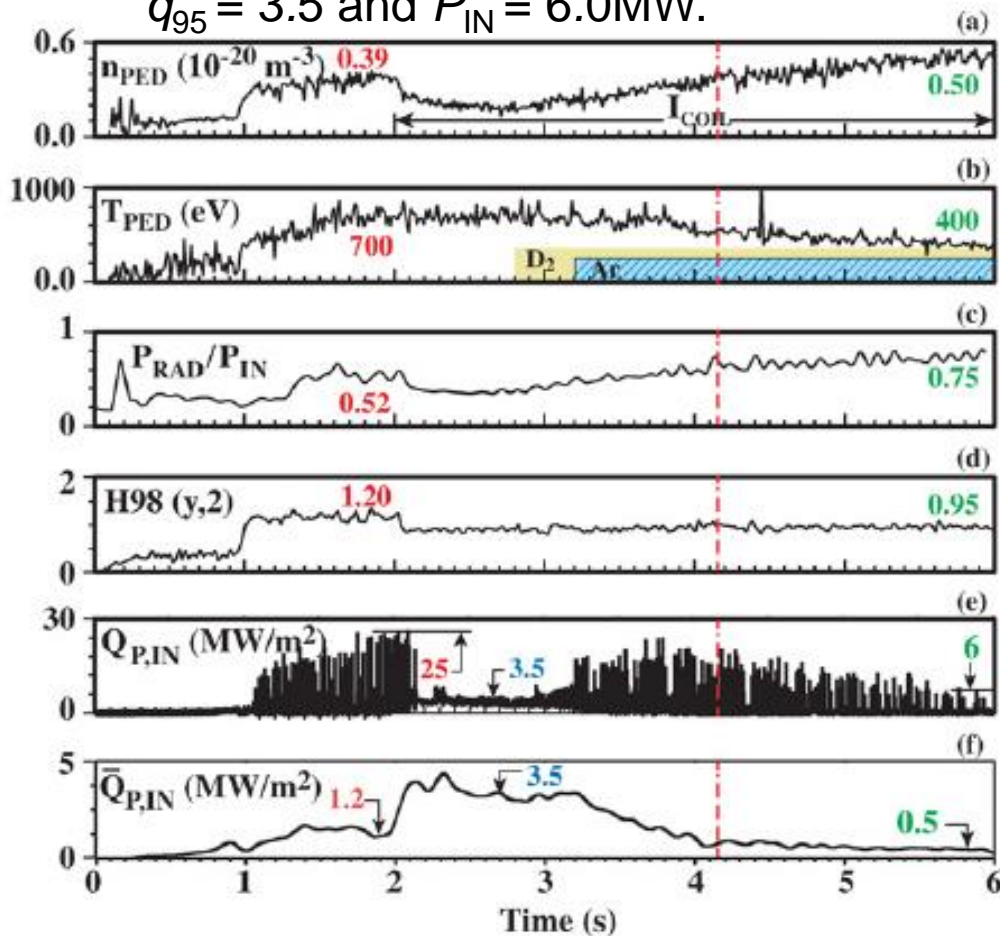
Recent result $n > 2n_G$!!

Lang Nucl. Fusion 52(2012) 023017

Results from radiating divertor experiments with RMP ELM suppression/control on DIII-D



Plasma parameters: $I_p = 1.43$ MA,
 $q_{95} = 3.5$ and $P_{IN} = 6.0$ MW.



- ✓ Under RMP ELM-suppressed conditions, divertor peak heat flux could be reduced by the addition of deuterium and argon gas puffing.
- ✓ The ‘cost’ in doing so, however, was triggering the return of ELMs, although these ELMs produced lower peak heat flux on divertor than that observed prior to the application of RMP.

T.W. Petrie, et al, Nucl. Fusion 51 (2011) 073003

- ✓ **ITER needs ELM control/suppression of Type I ELMs**
- ✓ **Linear stability boundaries are relatively well detected**
- ✓ **Nonlinear behaviour is important**
- ✓ **Possible control options**
 - ✓ ***Radiating divertors (type-III ELM)***, successful ELM control and full H-mode confinement have still to be demonstrated.
 - ✓ ***Magnetic triggering*** (“vertical kicks”) need in-vessel coils.
 - ✓ ***Pellet pacing*** can typically achieve a factor of two reduction in the energy per ELM – this is not enough.
 - ✓ ***External magnetic perturbation*** Very promising results up to now but physics is not clear
 - ✓ ***Combine methods*** have good future

Edge localized modes: recent experimental findings and related issues

Plasma Phys. Control. Fusion **49** (2007) S43–S62

**K Kamiya¹, N Asakura¹, J Boedo², T Eich³, G Federici⁴,
M Fenstermacher⁵, K Finken⁶, A Herrmann³, J Terry⁷, A Kirk⁸,
B Koch³, A Loarte⁹, R Maingi¹⁰, R Maqueda¹¹, E Nardon¹², N Oyama¹
and R Sartori⁹**

+ recent publications for control with external coils

Substantial amount of the material for this lecture was taken from the talks given by Yunfeng Liang and Howard Wilson on 480th Wilhelm and Else Heraeus Seminar on „Active Control of Instabilities in Hot Plasmas” (16-18 June, Bad Honnef, 2011)

- 1) We can not tolerate ELMs because
- 2) If we see ELMs we are in
- 3) Peeling and kink modes are essentially the same thing
 - Driven by density gradient, stabilised by gradient
- 3) Ballooning mode is unstable when critical gradient is sustained.
- 4) ELM control techniques are:
 -
 -